A CONTROL MODEL OF MUSCLE CONTRACTION

by

Brian P. Self

Thesis submitted to the Faculty of the

Virginia Polytechnic Institute and State University

in partial fulfillment of the requirements for the degree of

Masters of Science

in

Engineering Mechanics

APPROVED:

Dr. D.J. Schneck, Chairperson

Dr. J. Wallace Grant

Dr. H.H. Robertshaw

April, 1991

Blacksburg, Virginia

A CONTROL MODEL OF MUSCLE CONTRACTION

by

Brian P. Self

Dr. D.J. Schneck, Chairperson

Engineering Mechanics

(ABSTRACT)

A cascading series of control systems is developed which incorporates the molecular events that are currently thought to cause a muscular contraction. The model is developed with the hypothesis that a series of disturbing signals (or inputs) simply propagate faster than the respective controlling signals can correct for them. Transfer functions for each system are developed, with quantification derived for the excitation and the excitation-contraction coupling control systems. These latter systems include the release of acetylcholine into the synapse, the depolarization of the muscle membrane, and the release of calcium ions into the sarcoplasm. Expressions involving the energy processes, as well as the exact mechanism of the power stroke, are also developed. The systems involved are the Krebs cycle, thick and thin filament regulation, and the generation of a cross-bridge power stroke.

Acknowledgements

The author would like to thank all of the appropriate academic personnel and family members, and hopes he doesn't forget anyone. Thanks to Dr. Schneck, for always reminding me that good biomedical engineers are first and foremost engineers, and for providing guidance and direction during my academic career. Thanks to Dr. Grant, who helped me keep things in perspective, and to him and Dr. Robertshaw for always providing me with a good chuckle. The staff in ESM have been a huge help and have also become friends, particularly Duane, Paula, and Mara. Alan, who has been a good friend as well as a great illustrator, is also appreciated. The author would like to thank his wife Krystal, who makes it all worthwhile, and of course his kind and loving parents who always ask, "are you ever going to get out of school?" and his sister Heather too. Also the in-laws and my grandparents, aunts, uncles, etc. (sound like the Oscars?) And finally, I want to thank my Grandad, who gave me a shining example of the benefits of higher education.

Table of Contents

List of Illustrations

List of Tables

Chapter I - Introduction and Background

Introduction

Movements as precise and delicate as performing eye surgery to those requiring the brute force of a weight lifter are all developed by skeletal muscle. This force-producing tissue makes up 40-43 percent of the body's weight in man, and 23-25 percent of the weight in women (Schneck, 1991). Its functions include producing locomotion, helping to maintain body temperature through shivering, and assisting the return of venous blood to the heart through extravascular compression. By mass it is the most abundant tissue in the body, and by function it is one of the most important.

The importance of muscle introduces the desire to model and analyze its attributes. A computer model or simulation can enable researchers to determine the response of skeletal muscle when experimentation is either impractical or impossible. Laboratory exercises on human tissue are often undesirable or unethical. Many situations exist where it is necessary to predict how the musculoskeletal system will perform, most notably in sub-gravity space environments, in hyperbaric underwater exploration, and in high-gravity aeronautical maneuvers. The study of pharmaceutical agents and the cause and effect of musculoskeletal diseases would also benefit from an accurate mathematical model of muscular contraction.

In order to perform a mathematical analysis of muscle, an understanding of the controlling systems and physiology of contraction must be obtained. A systematic, accurate tabulation of the control systems within the contractile process should be devised. This should then be developed into a detailed control diagram of the physiological events which occur during muscular contraction. Many researchers have attempted to analyze muscle contraction, but to date there is no comprehensive, definitive model which is based on the molecular events which are thought to occur.

Historical Overview

The first major breakthrough in mathematically classifying muscle was made by A. V. Hill (1938). In this classic work, muscle heat measurements during various tetanized muscle experiments are measured by using a coupled galvanometer system. A tetanized muscle is the most active state that a muscle can achieve, and is capable of generating the largest force. Hill uses isometric experiments, where the muscle is not allowed to shorten, in conjunction with shortening trials where he varies the shortening lengths and the applied loads. He discovers that heat generated in excess of isometric exists in two independent forms. The first is a heat of shortening, which is found to be proportional to the amount of shortening and independent of load. The second form of excess heat is that of mechanical work, which is load-dependent.

If the muscle shortens by x cm, then the amount of shortening heat can be given as ax. a is the apparent internal resistance to shortening measured in gram-weight (gm-wt), which is the force applied to a one gram mass by a 1 g gravitational field. If the muscle shortens against a load P gm-wt, then the mechanical work is given as Px, in cm gm-wt. The total energy release of muscle contraction in excess of isometric (where $x = 0$) is given by $(P+a)x$. The rate of this energy release for an isotonic (constant load) contraction can be found by differentiating this quantity with respect to time, which yields $(P+a)v$ in cm gm-wt/sec, where

v is the speed of shortening in cm/sec. During experimentation, Hill (1938, p. 161) concludes that "the rate of extra energy liberation $(P+a)v$ is a rather exact linear function of the load P, increasing as P diminishes." He further finds that this rate is zero when the load P reaches the isometric load P_0. Assigning the rate of energy liberation as b cm/sec, a relationship can be written:

$$(P + a)v = b(P_o - P) \qquad [1]$$

By rearranging terms and noting that P_o, a, and b are all constant for a given muscle, the classic Hill equation is obtained:

$$(P + a)(v + b) = (P_o + a)b = constant \qquad [2]$$

Hill is able to obtain this result through precise heat measurements and careful experimental method. The remarkable fact is that the equation can be verified through mechanical experiments. Hill's equation accurately relates speed and load in an isotonic and in an isokinetic shortening, and the variables a and b match very closely for mechanical and heat experiments. The Hill equation has proven so successful that subsequent researchers have been prompted to apply the equation to their own results in order to validate their work. Unfortunately the equation does not fit well to a muscle during lengthening, and as stated previously the molecular mechanisms of muscle contraction were not considered in the analysis (and indeed at the time were almost totally unknown).

The sliding filament theory proposed independently by two teams of researchers, A.F. Huxley and Niedergerke (1954) and H. E. Huxley and Hanson (1954), greatly encouraged the field of muscular research. Many models now began to focus on the behavior of the myostructures referred to in the sliding filament theory, but still did not incorporate molecular events into their models. A common technique was to model the muscle using springs and dashpots.

Several such lumped-parameter models are shown in Figure 1. Green (1969) prefers the use of a modified-Voigt model in his analysis. This viscoelastic model assumes the parallel elastic element and the viscous element are neurally controlled. Bahler (1968) proposes an analysis in which the parallel elastic element present in most models is considered negligible. This assumption limits the model's applicability to stretches smaller than 1.2 times the resting length of the muscle. The contractile element is divided into a force generator and an inertial load function, in parallel with one another. The mathematical equation from this model is a third order polynomial, which does not coincide with the exponential function exhibited in the transition between rest and contraction. Bawa (1976) proposes a five-parameter model consisting of a series and a parallel elastic element, a viscous damper, and magnitude and rate constants for the decay of the active state. Finally, Schneck (1991) describes a fourth model, and also discusses a very early attempt by Nubar (1962) to model the tissue based on a constant volume analysis.

The familiar spring-dashpot approach is altered somewhat by Williams and Edwin (1970), who devise an electrical analog to the familiar lumped-parameter mechanical models. The energy stored in elastic springs is modelled as capacitance, the viscous energy dissipation is modelled as the energy lost to a resistor. Voltage and charge replace tension and displacement, and an energy conservation analysis is performed. FitzHugh (1977) applies two cost functions to the optimal control of muscle. The cost functions which are minimized are time and the total energy expenditure of the muscle. He includes only a contractile element in his model, in order to simplify the mathematical analysis. A discussion of the inclusion of other elements is also given.

The most complete myocybernetic model to date is proposed by Hatze (1981). He also utilizes a series of springs and viscous dampers to describe muscle, as shown in Figure 2. Hatze assumes that each contractile element in the fiber possess the same properties, and that all of the fibers in the model consist of identical components.

The contractile element is the only active element involved in Hatze's model. This element is dependent on five factors; the length of the sarcomere, the contractile history, the

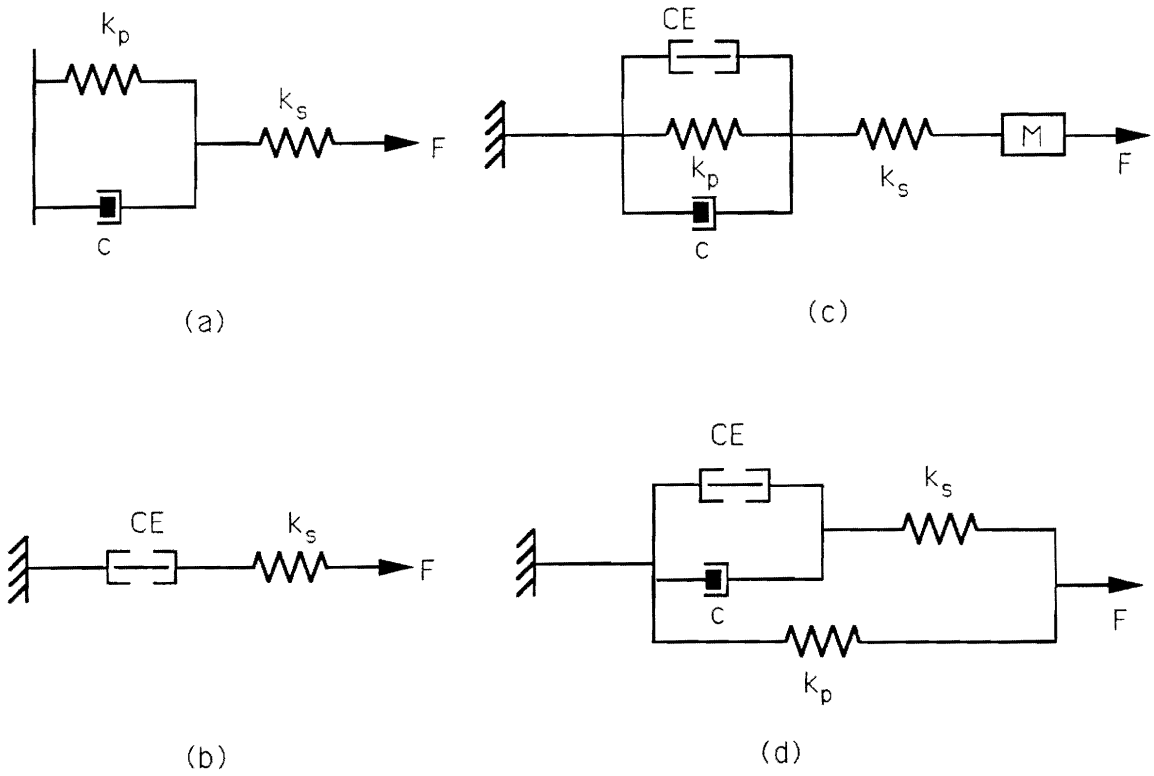

Figure 1. Spring-Dashpot Models: Diagrams of models used by (a) Green (1969), (b) Bahler (1968), (c) Bawa (1976) and (d) Schneck (1991), where c denotes a viscous damper, k_s a series spring, and k_p a parallel spring.

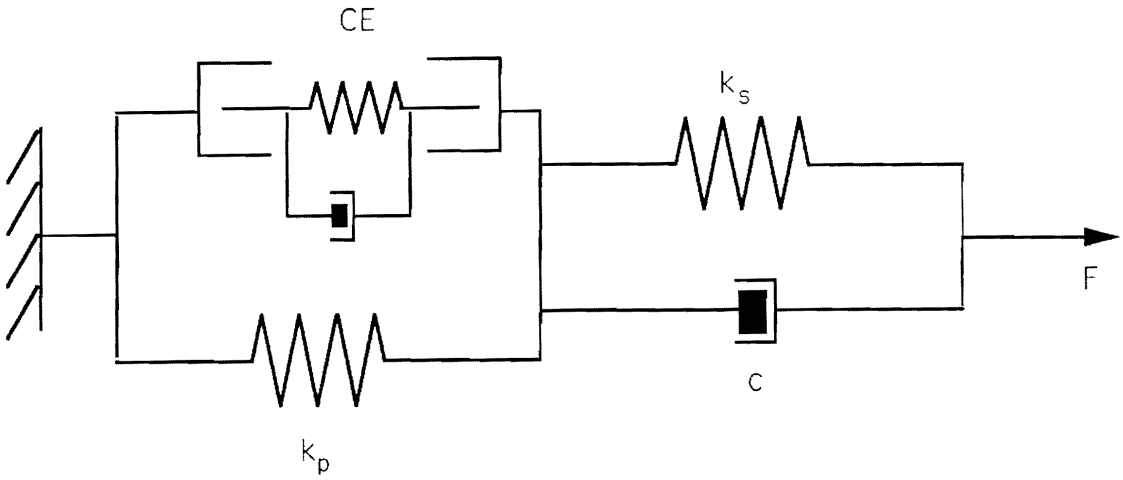

Figure 2. Spring-Dashpot Model of Hatze: The model used by Hatze consists of a contractile element with inherent elasticity and viscosity, along with a viscous damper, a parallel spring, and a series spring (from Hatze, 1981).

speed of shortening, the degree of stimulation, and the temperature. These factors all affect the contractile element nonlinearly. The five controlling factors are then simplified into three basic functions, consisting of an active state function, the degree of filamentary overlap, and the velocity of lengthening or shortening.

Hatze assumes that each cross-bridge exerts an "average contractive force", which is primarily dependent on the velocity of contraction. This average force is denoted by the function $G(\dot{\lambda})$, where λ represents the instantaneous length of the sarcomere. The number of cross-bridges active at any one time is dependent on the three factors mentioned above. The fraction of active cross-bridges is denoted as Ω, while the total number of cross bridges in a half sarcomere is denoted by N. Thus the force output of the contractile elements is

$$f^{cp} = N\Omega G(\dot{\lambda}) \qquad [3]$$

The fraction of active cross-bridges Ω is postulated to be dependent on the active state q, the normalized degree of filamentary overlap k, and the normalized velocity of shortening/lengthening H.

Hatze then derives equations for these parameters. The active state function is dependent on the amount of calcium present in the sarcoplasm (denoted as γ), which is in turn dependent on the action potential (or β) of the sarcolemma and the T-system. A wonderful mathematical model of the contraction of a single muscle fiber is then derived. Unfortunately, in Hatze's following chapter, the entire model is virtually abandoned for a simpler, more global analysis of the human musculoskeletal system. To his credit, Hatze was attempting to perform an overall analysis of the human body. Unfortunately, his final results do not deviate greatly from work previously performed.

Once again, this evaluation of muscle contraction does not delve into the control systems present in the tissue. Hatze (1981, p. 16) even states himself that "it is intended to simulate the functional control behavior of the muscle as a driving-structure in the link system of the animal, an aim that precludes modelling at the molecular level as irrelevant to the problem

at hand." Hatze's model does, however, seem to be the classic work to date in the field of myocybernetics. Little has been done since then that greatly refutes or replaces his efforts.

Most of the models presented fit experimental results reasonably well, at least for specific conditions. Yet each has its miscomings, and none seem to capture the molecular mechanisms of muscle contraction. Perhaps Green (1969, p. 41) words it best when he realized that "if the characteristics of each subsystem and the rules for connecting one component to another were completely known, the problems would effectively be solved."

Anatomy of Muscle

In order to construct an accurate control diagram of muscular contraction, the structure of muscle must be explored. The reader is referred to several excellent texts on the anatomy of muscle for an indepth analysis of the tissue structure (Squire, 1981; Woledge et al., 1985; Guyton, 1986; Schneck, 1991). The values used in this section are a synopsis of measurements quoted in these references. Muscle is made up of several hundred to several thousand muscle fibers, each of which is actually a single, multi-nucleated cell. These cells contain structures similar to other cells, including vast numbers of mitochondria which provide energy for contraction. The cytoplasm of the cell, or its intracellular fluid, is known as sarcoplasm (or myoplasm) and is high in potassium, magnesium, phosphate, and protein enzymes. The sarcoplasm is contained by an outer membrane known as the sarcolemma. An extensive intracellular membranous structure known as the sarcoplasmic reticulum is also present in the cell, and runs mostly parallel to the axis of the fiber. A second membranous structure, consisting of the transverse tubules, runs perpendicular to the axis of the fiber. This T-system is actually continuous with the sarcolemma, and (like the sarcolemma) is an excitable membrane. These structural components of the muscle cell (and muscle fiber) are shown schematically in Figure 3.

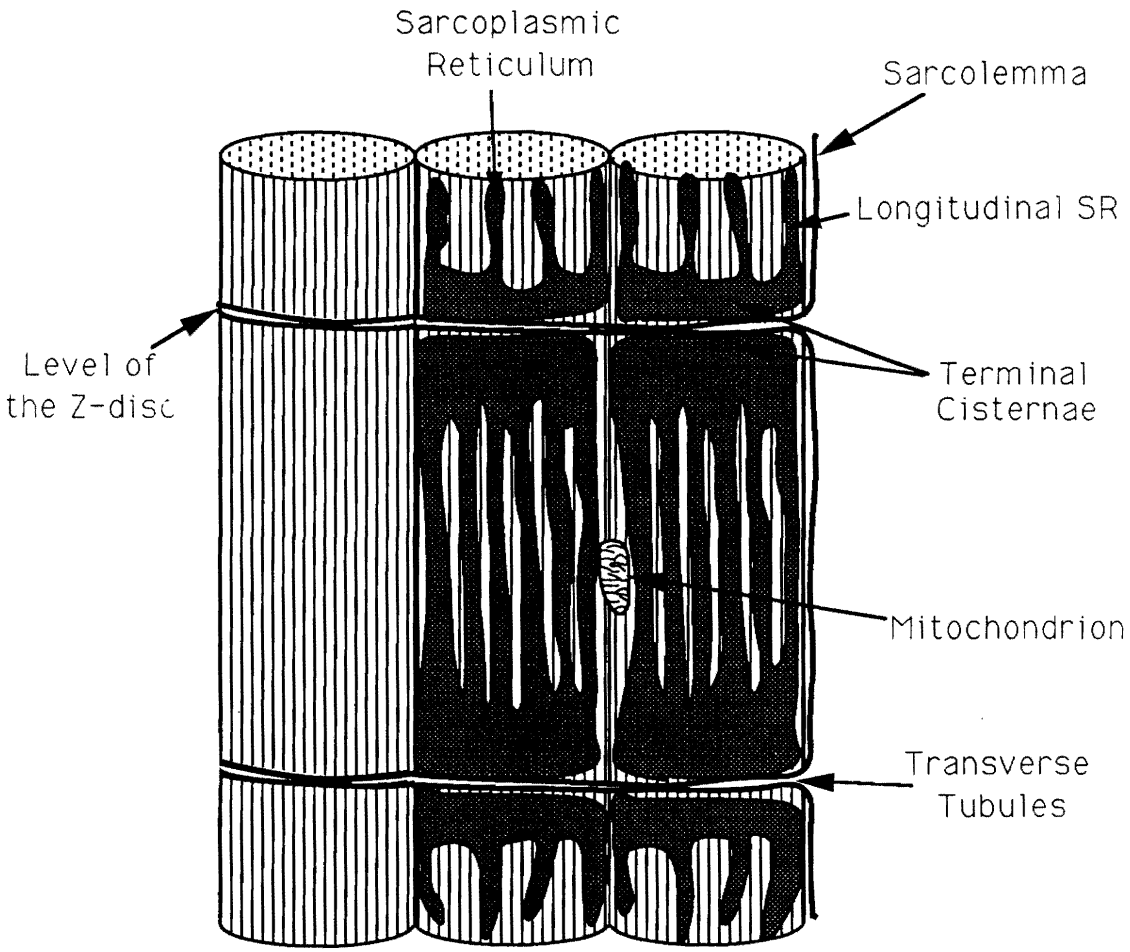

Figure 3. Anatomy of Muscle Fibers: The various components of a muscle fiber, including the sarcolemma, the T-tubules, mitochondria, and the longitudinal and terminal cisternae portions of the sarcoplasmic reticulum (after Guyton, 1986).

Each muscle fiber is composed of several thousand subunits known as myofibrils. These are the smallest naturally occurring structures which have exhibited contraction, and are thus often referred to as the contractile elements of muscle. The myofibrils run in parallel units down the axis of the muscle fiber, and are interconnected by a membranous structure known as the Z-disc. The myofibrils can be further subdivided into the fundamental structural unit of the muscle, the sarcomere.

The structure of the sarcomere was discovered by studying light microscopy images of muscle. These images have long been known to display repetitive units of light and dark bands, as shown in Figure 4. The dark bands, known as the A-bands, are anisotropic to polarized light. The I-bands, which are isotropic to polarized light, appear lighter in the diagram. Finally, a dark line known as the Z-line can be seen dividing the I-bands. The area between two successive Z-lines (which are caused by the Z-discs) is known as the sarcomere.

The striations in the microscopic images were proven to be due to different protein structures present in the muscle tissue. The repeating unit of the sarcomere can be broken down into two main constituents, the thick and the thin filaments. The thin filaments are attached to the Z-disc, the protein membrane which passes through the entire cross-section of the fiber. The thick filaments are positioned in the center of the sarcomere. The area where the thick and thin filaments overlap is anisotropic to polarized light, thus creating the A-band. The thin filament alone, however, is isotropic to light and gives rise to the I-band. It is by studying these bands during contraction that the sliding filament theory of muscle contraction was postulated (to be discussed later).

The thick filament is composed of strands of myosin, a complex protein with a molecular weight of around 450,000 daltons (1 dalton = 1.66024×10^{-24} grams). The myosin molecule is approximately 1500 Angstroms long and consists of two heavy and four light chains. The light chains compose the tail of the protein structure, while the head of the molecule is formed by the heavy chains. This head is composed of two globular subunits, known as HMM S-1 and HMM S-2. Close to the region where these two units join are molecules known as regulatory light chains. They are thought to exhibit some control over the force of the contraction. The

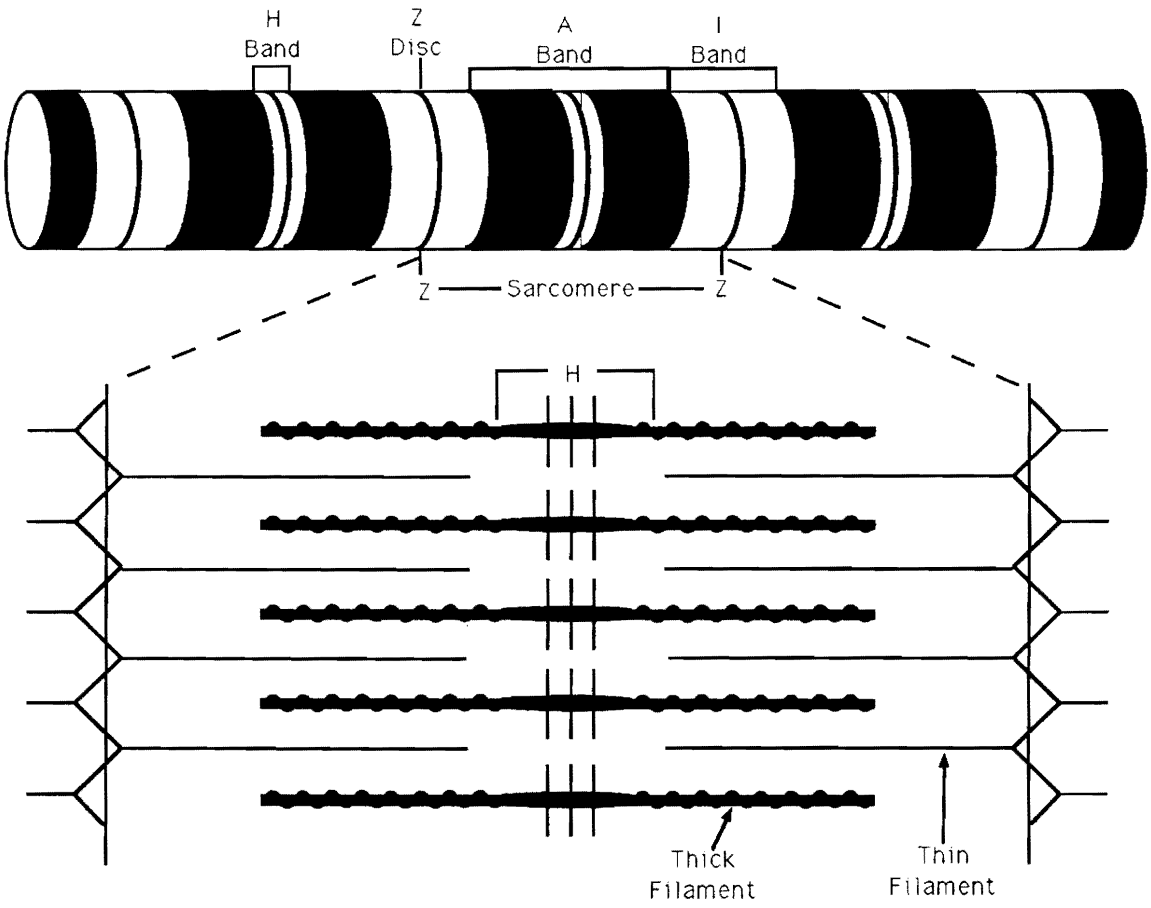

Figure 4. Striations of Muscle Tissue: The characteristic striations of muscle cells are due to the distribution of thick and thin filaments (after Guyton, 1986).

HMM regions exhibit ATP-ase activity, or will catalyze the breakdown of adenosine triphosphate (ATP). This reaction provides energy for contraction. The structure of the myosin molecule is shown schematically in Figure 5(a).

Anywhere from 100 to 250 of the myosin tails are intertwined in a helical structure to form the thick filament. The heads of the myosin molecule extend outward from the tails and main body of the helix, as shown in Figure 5(b). The period of the helix is approximately 429 Angstroms, which corresponds to a set of three myosin heads spaced sixty degrees apart for each period, or one pair of myosin heads every 143 Angstroms. In the middle of this helix, only the tails of the myosin molecules are present. This area is known as the H-zone and consists of a length of about 0.15 microns where the thick filaments contain no myosin heads.

The thin filaments, shown schematically in Figure 6, are composed primarily of the protein actin. Two F-actin molecules intertwine to form a helical structure with a pitch of approximately 70 nm. Each pitch contains thirteen to fourteen subunits of G-actin, which corresponds to a length of 55 Angstroms per subunit. Each of these subunits contains one molecule of ADP, and it is thought that this is where the active site of the actin is located. Two other constituents make up the thin filament. The first is tropomyosin, which is a double protein strand with a molecular weight close to 70,000 daltons and a length of 40 nm. About two-thirds down the length of each tropomyosin molecule is a group of proteins known as troponin. Three different forms of troponin exist in the thin filament. Troponin-C binds strongly to calcium ions, while troponin-T binds to the tropomyosin. Troponin-I has been found to inhibit cross-bridge formation even in the absence of coupling with tropomyosin. Troponin and tropomyosin have been shown to be important in the regulation of muscle contraction.

Physiology of Muscular Contraction

The physiology of muscle is inherently linked to its structural components. Several works discuss the steps of muscular contraction, including Guyton (1986), Woledge (1984), Squire

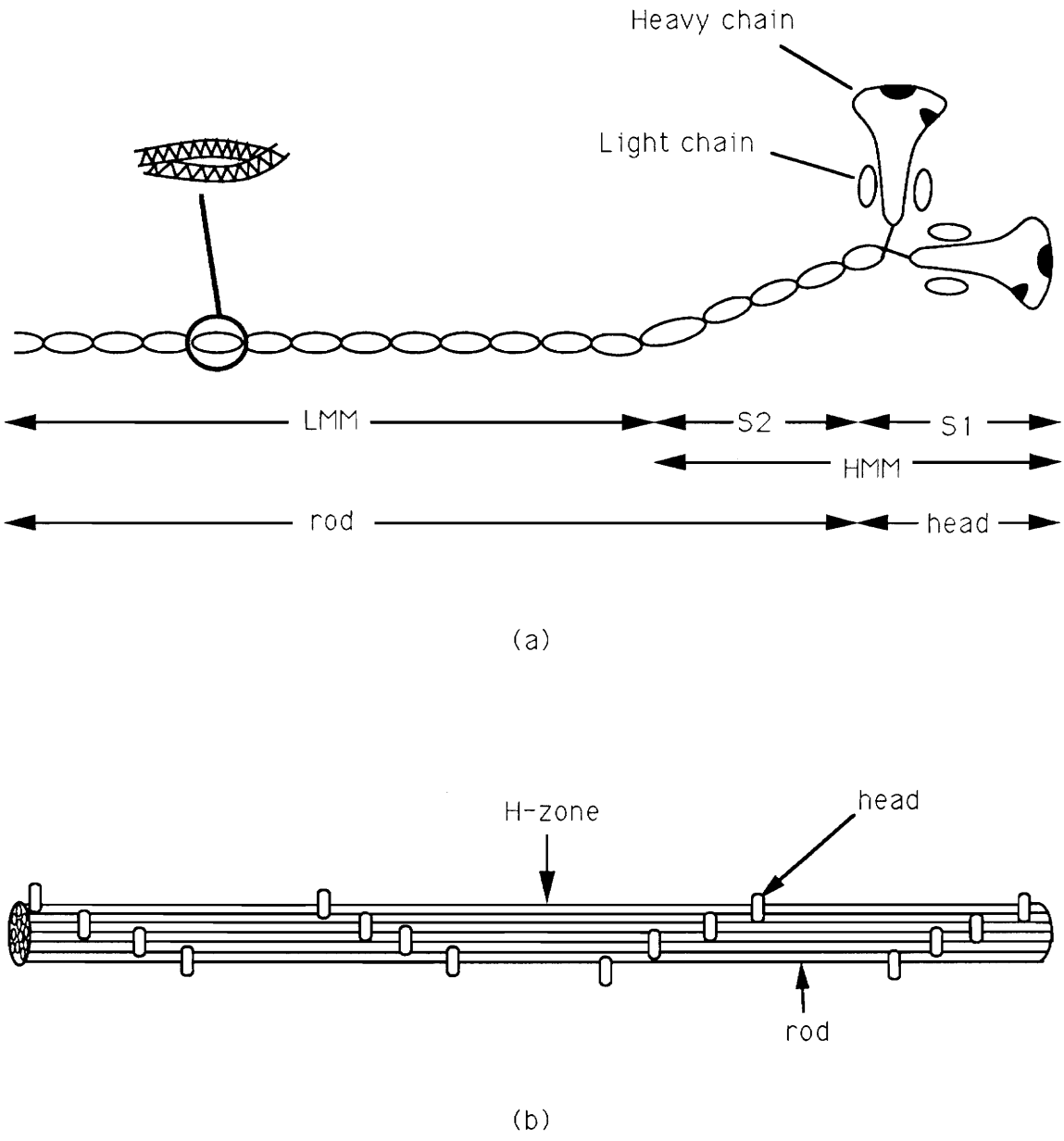

Figure 5. The Myosin Molecule and the Thick Filament: (a) The structure of the myosin molecule found in skeletal muscle and (b) their formation of the thick filament (after Bagshaw, 1982).

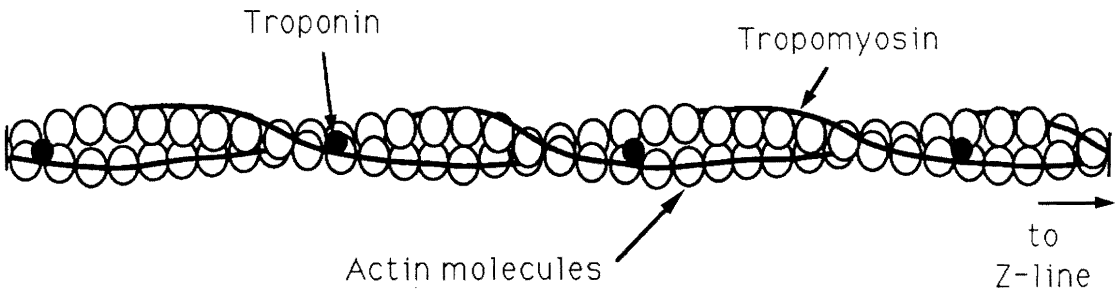

Figure 6. The Thin Filament: The thin filament consists of a double helix of actin intertwined with tropomyosin strands and periodic troponin molecules (after Guyton, 1986).

(1986), and Bagshaw (1982). The initiation of a muscular contraction is a nervous impulse from the α-motor neuron. The impulse releases acetylcholine (ACh) into the neuromuscular junction, where the motor neuron and the sarcolemma join. The ACh binds to receptor cells on the surface of the muscle membrane, which triggers an action potential that propagates along the longitudinal axis of the muscle fiber. This depolarization travels laterally through the transverse tubules, which come into contact with the sarcoplasmic reticulum at a junction known as the triad.

When the muscle action potential reaches the triad, it is somehow transmitted to the cisterns of the sarcoplasmic reticulum. These cisterns contain large amounts of calcium ions and upon excitation, release some of the ions into the sarcoplasm. If successive stimuli occur (generally around 4 Hz), the level of Ca^{++} will reach a threshold and initiate the contractile process. The calcium ions perform two functions. The first is to bond to the troponin-C molecule of the thin filament. This somehow releases the inhibitory effect which tropomyosin imposes upon the bonding of actin and myosin. The prevailing theory, known as the steric blocking model, is that the Ca^{++} causes a conformational change in the troponin-tropomyosin complex, which then uncovers the active sites on the actin monomers. This mechanism is known as the "protein switch" of muscle contraction (Cohen, 1975) and is shown schematically in Figure 7. Recent evidence seems to indicate that the Ca^{++}-activated tropomyosin may actually activate the ATP-ase activity of the myosin cross-bridge (see Squire, 1989). Whichever mechanism occurs, the Ca^{++} is responsible for the activation of the troponin and tropomyosin. The second contribution of Ca^{++} is to aid in the splitting of ATP on the myosin head. The ion is thought to bond lightly to the top of the HMM S-1 chain, which changes the electrical charge distribution of the myosin head. The head then changes its configuration, which brings the ATP into close contact with the ATP-ase region of the myosin. This causes the ATP molecule to be hydrolyzed, which releases energy to drive the contraction and removes the ATP inhibition of the formation of the actomyosin complex.

When the inhibitory effect of the ATP and of the tropomyosin is removed, the myosin head is free to bond with the actin monomers. This connection between the thick and thin filaments

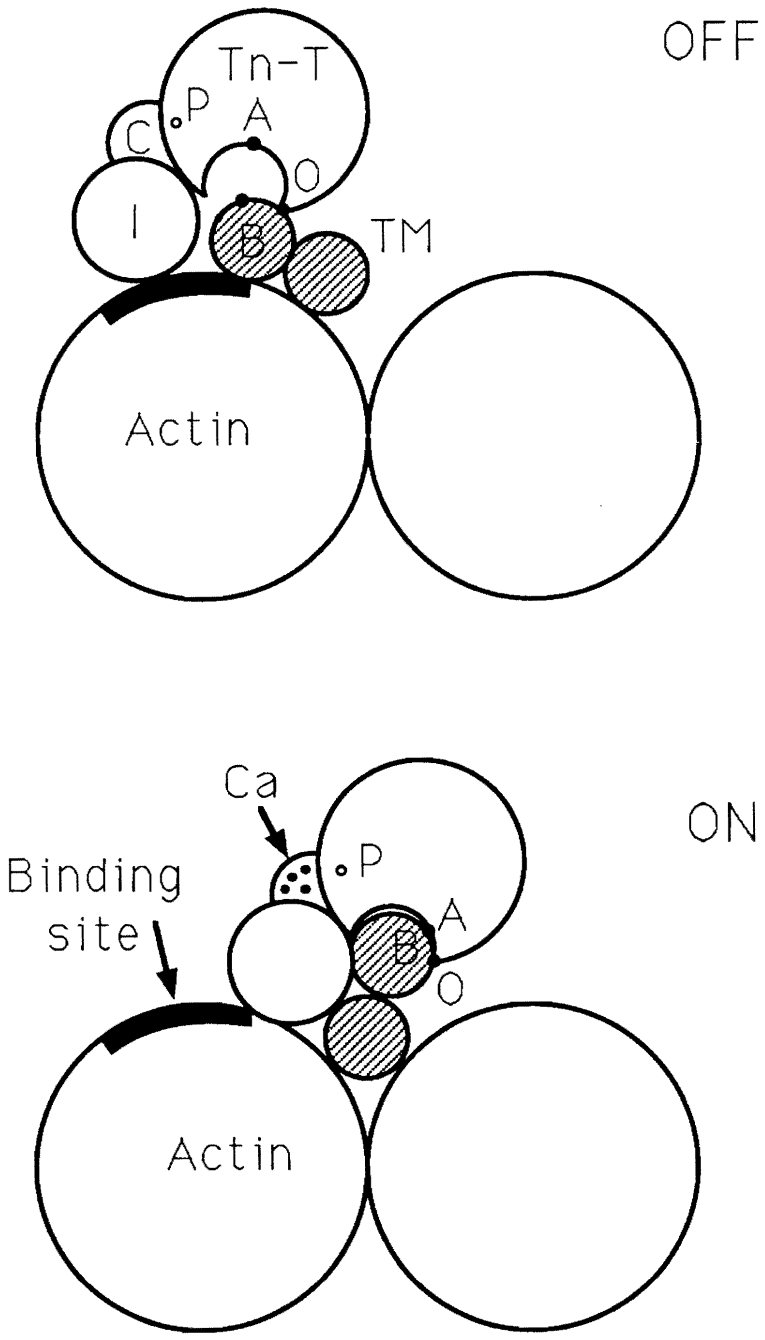

Figure 7. The Steric Blocking Model: The TnC-Ca^{++} complex causes a conformational change in the tropomyosin strands, which uncovers the site on the actin molecule (after Squire, 1989).

is known as a cross-bridge. Electromagnetic forces (which are not fully understood) and energy released from the hydrolysis of ATP are thought to cause the cross-bridges to rotate towards the center of the thick filament. This rotation causes a translation of the thin filaments attached to the cross-bridges. In this way the Z-discs are pulled closer together, and a contraction occurs.

As the contraction is taking place, the Lohman reaction resythesizes a molecule of ATP. This ATP then bonds to the myosin head which has a dissociation effect on the actomyosin complex. Energy released by the ATP may also actively aid in the release of Ca^{++} from the troponin, which induces the breakdown of the cross-bridge. Accompanying these affects is an increase in the strain of the myosin head. As the cross-bridge "rotates", the mechanical stresses approach the bond strength of the actomyosin complex. These three factors, i.e. (1) the resynthesis of an ATP molecule on the myosin head, (2) the dissociation of Ca^{++} from troponin, and (3) the mechanical stresses induced in the cross-bridge, combine to cause the breakdown of the actomyosin complex. From microscopic studies of fully contracted insect flight muscle, the angle at which this occurs is thought to be about 45 degrees off of the axis of the thick filament (Reedy, 1965). Once the bond is broken, elastic restoring forces (and possibly electromagnetic and thermodynamic field effects) return the cross-bridge to its equilibrium position of approximately 90 degrees to the axis of the thick filament. Now the ATP-bound myosin head is prepared for the next cross-bridge cycle.

Hundreds of these cross-bridges are forming asynchronously as a muscle contracts. While intact cross-bridges hold the thin filaments in place, new cross-bridges are being formed which will bond to new actin active sites. In this way the thin filaments will "walk along" with respect to the thick filaments, and a contraction will take place. This is shown diagrammatically in Figure 8.

A single nervous impulse will cause the described events to occur in an all-or-none fashion; the impulse (if strong enough) will elicit a muscle action potential, which will release a certain amount of Ca^{++}. If it is above the threshold concentration, the Ca^{++} will induce the formation of the actomyosin complex (the cross-bridge), and a contraction will occur. Relax-

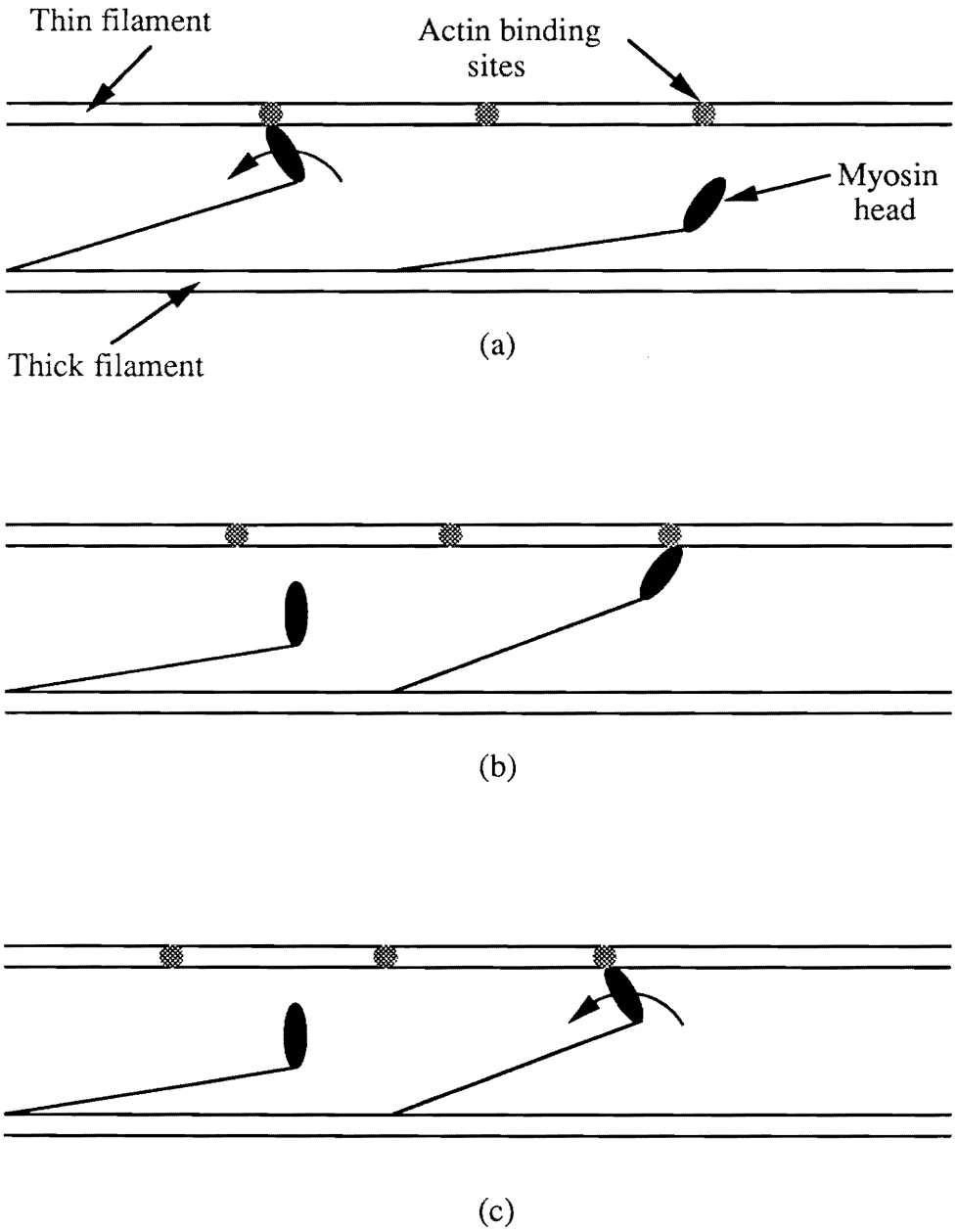

Figure 8. The Ratchet Action of the Cross-Bridges: The proposed position of the cross-bridges, whereby (a) a cross-bridge produces a power stroke, then (b) detaches and another cross-bridge attaches, then (c) produces a second power stroke.

ation consists of the repolarization of the sarcolemma and the transverse tubules, of the binding of an ATP molecule on the myosin head, and of the resequestering of Ca^{++} in the cisterns of the sarcoplasmic reticulum.

If a second nervous impulse stimulates the muscle fiber before relaxation is complete, a phenomenon known as wave summation takes place. The impulse will cause a release of Ca^{++} ions which will add to the amount already present in the sarcoplasm (initial release minus the amount resequestered). The larger concentration of Ca^{++} will then result in a greater number of active actin sites, or a higher "active state" of the muscle fiber. Each successive stimulus will add to the amount of Ca^{++} present in the sarcoplasm, thus increasing the number of attached cross-bridges. If the stimuli are applied at higher and higher frequencies, a limit will be reached where all of the available Ca^{++} has been released. This limit is described as tetanus, the maximum active state of a muscle fiber. Since the number of attached cross-bridges controls the amount of force a muscle can generate, tetanus also describes the maximum force output of a muscle fiber.

The physiology of muscle contraction is still not entirely understood. The exact mechanism of the generation of force by the cross-bridges is being heavily investigated. The present theories seem to explain experimental results well, and the sliding filament theory has survived for the past thirty years. By utilizing the existing theories of muscle contraction, it is possible to construct a control diagram. A control model of the mechanics of muscle contraction would quantify the action of muscle, and possibly indicate the direction for further research in the molecular events of muscular contraction.

Chapter II - Problem Statement

Most contractile models to date have been myocybernetic, lumped-parameter representations, treating the muscle as a "black box." These models are not based on theory or microstructure, but are simply curve-fitting equations to responses seen in muscle experiments. These models also make it difficult to study variations in any of the parameters which affect the many steps of muscle contraction, such as the effect of altering the concentration of calcium or of the variations of cross-bridge activity. This study begins the development of a control model which incorporates the molecular events that are thought to occur during muscular contraction, from which deductive constitutive behavior of muscle tissue may be surmised. An α-motor neuron impulse will be the primary input to the system, with other parameters assumed to be at normal, healthy values. The response of a single muscle fiber shall then be discussed, which will include Ca^{++} concentrations, pump rates, and various physiologic transfer functions.

A brief description of the phenomena associated with muscle contraction was given in Chapter 1, accompanied by a short synopsis of previous attempts to model it. A detailed control diagram of the molecular events leading to the contraction of a muscle fiber shall be presented in Chapter 3, accompanied by a description of possible transfer functions. Finally,

a summary of the analysis, conclusions obtained from the control model, and the direction of future studies will be offered in Chapter 4.

Chapter III - Control Model

Control diagrams are often used in the field of engineering. No more sophisticated control systems exist than those present in the human body. Yet they can all be reduced to a fundamental canonical form, consisting of a controlling system, a controlled system, a disturbing signal u_d, a control signal u_c, a reference signal u_r, an output u, and a primary feedback signal u_p. These are shown in the standard control diagram of Figure 9. A general description of this single feedback control system is given in Appendix A.

Muscle contraction as a whole can also be incorporated into this diagram, as shown in Figure 10. The controlled system is the muscle itself, while the controlling system is the motor cortex of the brain. It is through the motor cortex that the "will" of the subject is exerted over his/her muscle tissue. The reference signal for the motor cortex is the "desired activity" of the muscle. Using this reference, the motor cortex establishes a controlling signal over the muscle tissue, which is a frequency of stimulation f_α. The muscle is disturbed by the external load against which it contracts, or, in the case of the myotatic reflex, by a passive stretch of the intrafusal muscle fibers. The tissue then combines the effects of the disturbance (the external load) and the control signal f_α. The output of the muscle is its actual activity, which is manifest as a displacement δ, a velocity $\dot{\delta}$, a force F, the time derivative of the force $\dot{F}$, and possibly higher order derivatives as well. This activity then proceeds through a feed-

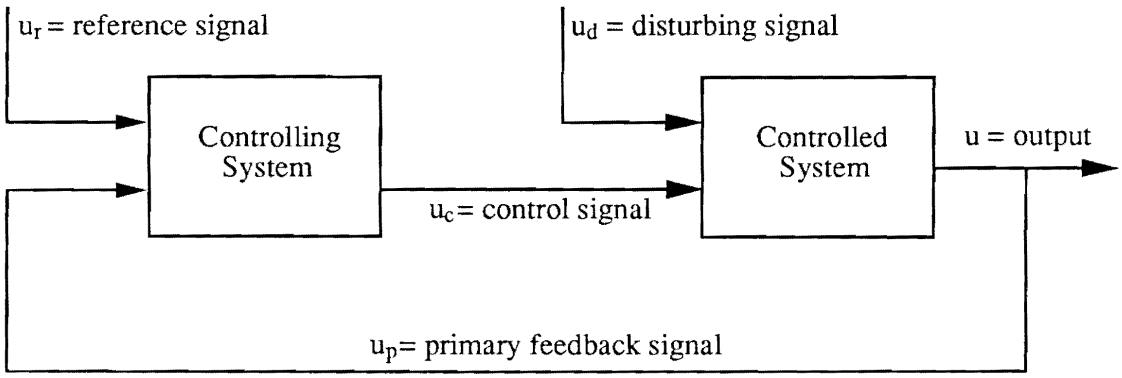

Figure 9. Generic Control Diagram: A control system consists of a controlling system, a controlled system, a disturbing signal u_d, a control signal u_c, a reference signal u_r, an output u and a primary feedback signal u_p.

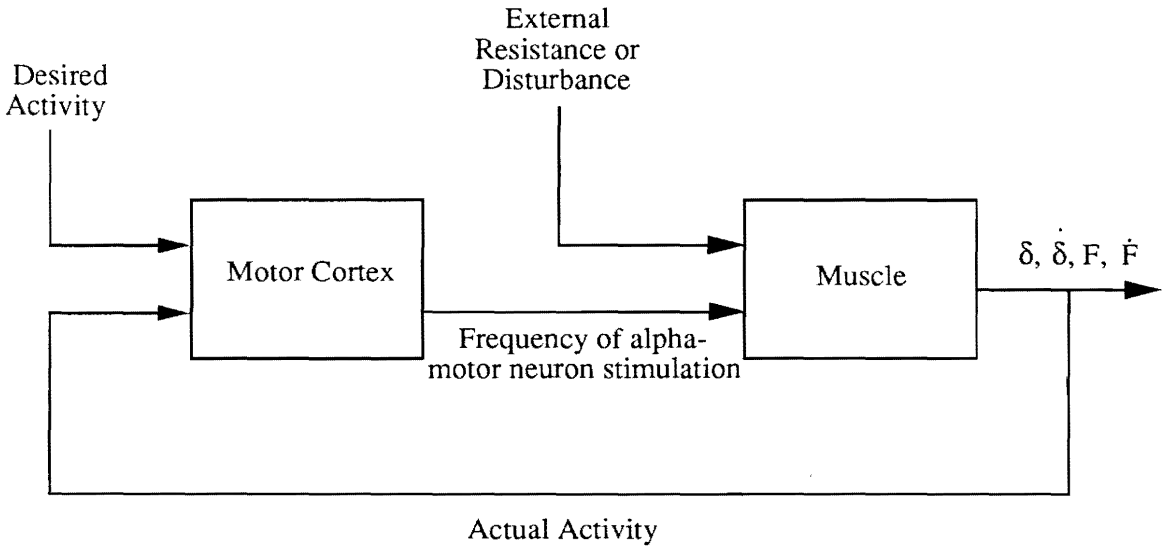

Figure 10. Overall Control Diagram of Muscle Contraction: This control model describes the neural inputs and performance feedback signals of the muscle as a whole, where u_d is the external load, u_c is the frequency of stimulation f_α, u_r is the "desired activity" of the muscle, and u and u_p are δ, $\dot{\delta}$, F and $\dot{F}$.

back loop to the motor cortex. The present project will model the controlled system of Figure 10 (the muscle), and will thus be a series of control systems within the overall control system of muscle contraction.

We shall proceed with the supposition that the impulse from an α-motor neuron perturbs the resting state of the tissue, and contraction results from a cascading series of disturbances that propagate faster than the embedded controlling signals can correct for them. Thus, all of the control systems described below are presumed to have as their ultimate objective a return of the anatomical architecture to some pre-existing resting configuration. For example, the sodium-potassium pump tries to repolarize the sarcolemma just as soon as the ACh causes a depolarization, and the Lohman reaction attempts to resynthesize an ATP molecule on the myosin head just as soon as the cross-bridge is formed. In this way it is possible for the muscle to attain a number of consecutive contractions. The cascading series of control diagrams for muscle contraction are shown in Figure 11. The controlling systems, controlled systems, and the various signals of muscle contraction are displayed in Table 1, from which the analysis follows.

Synaptic Transmission

The first control system, shown in Figure 12, is initiated by the release of acetylcholine (ACh) from the synaptic terminals of the α-motor neurons. As previously mentioned (and illustrated in Figure 10), the motor cortex receives an input of some "desired activity" and sends an impulse down the α-motor neuron. Several methods can be used to quantify the stimulating pulse, including half-sine waves (Hatze, 1981) and Fourier analysis. Hatze uses a function where each impulse i arrives at time t_i, where $i = 1, 2, 3....$ The amplitude of the impulse is given as $V_N\alpha(t)$, where V_N is the resting voltage (about - 90 mV) and $\alpha(t)$ is a half-sine wave of half-period 1 msec given by:

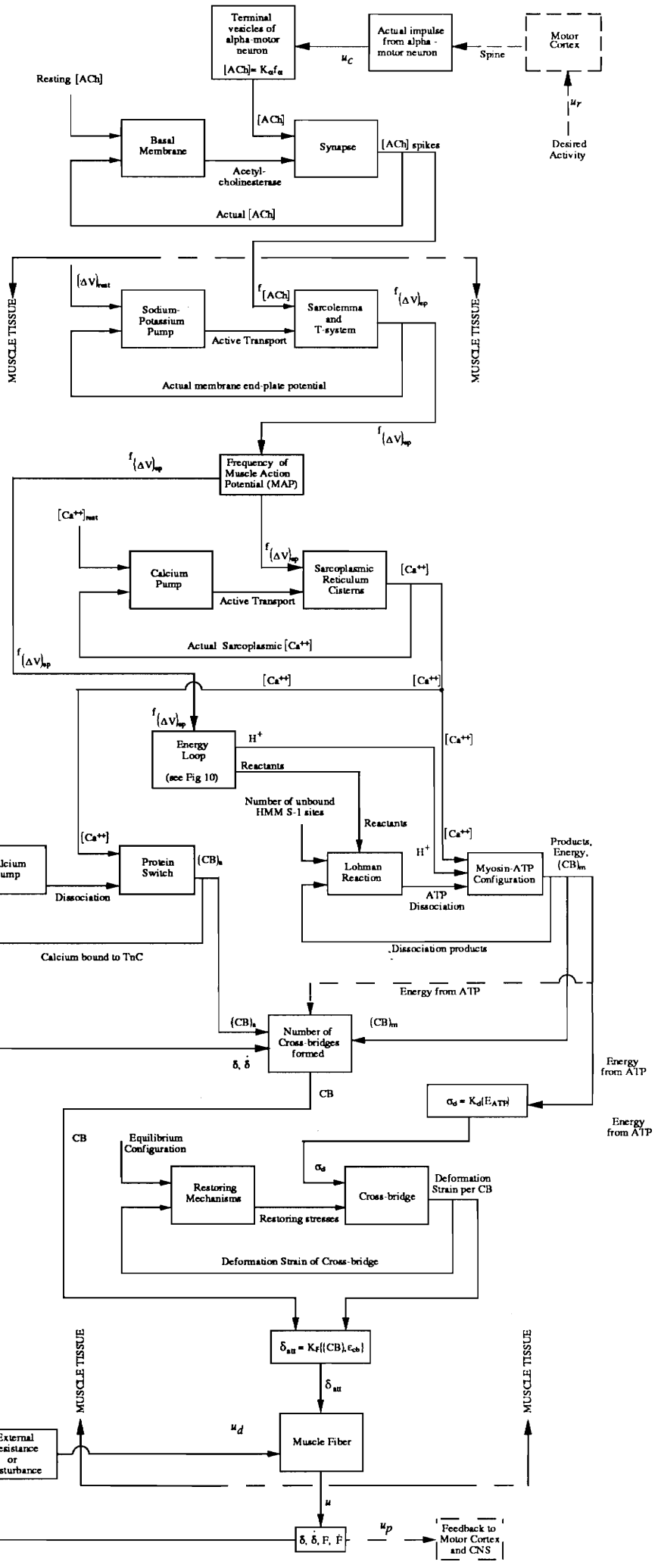

Figure 11. Control Model of Myofibrillar Contraction: The cascading series of control systems for muscle contraction.

Table 1. Control Systems of Muscle Contraction

Event	Controlling System	Controlled System	Control Signal, u_c	Reference Signal, u_r	Disturbing Signal, u_d	Output and Feedback, u
(a) Release/ Synaptic Tranmission of ACh	Basal Membrane	Synapse	Activity of Acetylcholin-esterase	Resting ACh (~ 0)	ACh release due to f_α	Actual [ACh] in the Synapse
(a) Depolarization of Muscle Membrane	Sodium-Potassium Pump	Sarcolemma and T-system	Active Transport of Na and K	Membrane Potential at rest (~ -90 mV)	ACh spikes	Propagation of muscle action potential
(b) Hydrolysis of water	Mitochondria	Water	Activity of Krebs Cycle Enzymes	Resting pH and water concentration	Frequency of muscle action potential	Release of Hydrogen Ions
(b) Hydrolysis of ATP	Mitochondria	Adenosine Triphosphate	Activity of Krebs Cycle Enzymes	Resting [ATP]	Hydrogen Ions	Reactants and Free Energy
(c) Release of Calcium	Calcium Pump	Sarcoplasmic Reticulum Cisterns	Active Transport of Ca^{++}	$[Ca^{++}]$ at rest (~ 10 nM)	Frequency of muscle action potential	Actual $[Ca^{++}]$ in the sarcoplasm
(d) Thin Filament Regulation	Calcium Pump	Protein Switch, TnC-bound Ca	Dissociation of TnC-Ca	$[Ca^{++}]$ at rest (~ 10 nM)	$[Ca^{++}]$ in the sarcoplasm	Available CB binding sites on actin
(d) Thick Filament Regulation	Lohman Reaction	Myosin-ATP Configuration	ATP dissociation effect on the cross-bridge	Number of unbound HMM S-1 sites at rest	Hydrogen and Calcium Ions	Energy, $(CB)_m$, P_i and ADP
(d) Power Stroke	Various Restoring Mechanisms	Cross-bridge	Various Restoring Stresses	Equilibrium Stresses at Rest (~ 0)	Deformation Stress From ATP Energy	Deformation Strain

(a) Excitation Control Systems
(b) Energy Loop Control Systems
(c) Excitation-Contraction Coupling Control System
(d) Contraction Control Systems

$$\alpha(t) = \sin 1000\pi(t - t_i) \quad for \quad t_i < t < (t_i + 0.001) \qquad [4]$$

If time t is not between t_i and $(t_i + 0.001)$, then $\alpha(t) = 0$.

Another common practice for analyzing biological signals is through Fourier analysis. This process assumes that any signal can be written as a sum of individual sine and cosine waves, each with a different amplitude and frequency. Any waveform with period T_P can be written as

$$u(t) = \frac{a_o}{2} + \sum_{n=1}^{\infty} [a_n \cos(2\pi n f_1 t) + b_n \sin(2\pi n f_1 t)] \qquad [5]$$

where $f_1 = 1/T_p$, n denotes each individual sine or cosine function, and the constants a_n and b_n are given by

$$a_n = \frac{2}{T_p} \int_0^{T_p} u(t) \cos(2\pi n f_1 t) dt \quad for \quad n = 0, 1, 2... \qquad [6]$$

$$b_n = \frac{2}{T_p} \int_0^{T_p} u(t) \sin(2\pi n f_1 t) dt \quad for \quad n = 1, 2, 3... \qquad [7]$$

This fourier transform can then be analyzed according to frequency and amplitude content (see Bendat and Piersol, 1971).

Dayhoff (1990) suggests that the muscle acts by recognizing certain patterns of impulses, or specific pulse trains. We shall simply assume a series of step impulses, arriving at a uniform frequency f_α. The signal propagates along the entire length of the motor neuron until it reaches the neuromuscular junction, or synapse, where the nerve and the muscle membrane meet.

The motor neuron branches into several different nerve terminals, which are collectively called the motor end plate. These nerve endings never actually come into physical contact

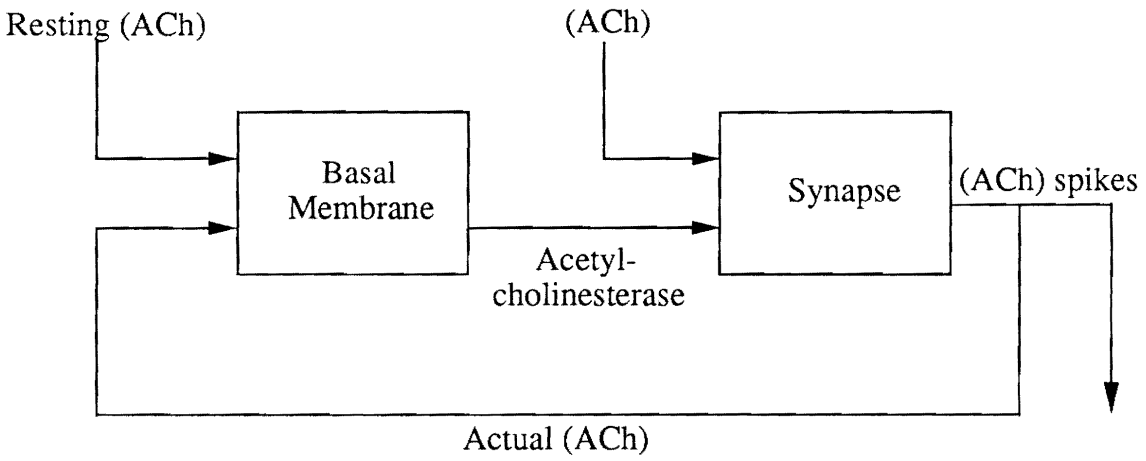

$$u_d = 10^{-17} \text{ moles of ACh per impulse}$$

$$u_r = 0 \text{ moles ACh}$$

$$u_c = \exp(-1/\tau_s), \text{ hydrolysis rate}$$

$$u = \text{ACh} = \sum_{j=0}^{f_\alpha} 10^{-17} \exp(-1/\tau_s (t - j/f_\alpha))$$

or

$$u = \text{ACh} = \sum_{j=0}^{f_\alpha} \int_0^t 10^{-17} \delta(t_f - j/f_\alpha) dt$$

Figure 12. Acetylcholine Release: The controlled system is the synapse, the controlling system the basal membrane. $u_d = 10^{-17}$ moles of ACh released per impulse, $u_r = 0$ moles of ACh, u_c is effectively τ_s, and u is given by equation [9] or [11], or by the frequency of ACh spikes.

with the muscle membrane, but are surrounded by an indentation in the sarcolemma known as the synaptic trough. Within the indentation there are a number of subneural clefts, which are small invaginations which increase the surface area of the neuromuscular junction. A basal membrane (the controlling system) containing acetylcholinesterase is also present within the synapse.

Plonsey (1969) describes the events that occur in the synapse as follows. The nerve terminal contains up to 300,000 synaptic vesicles, each containing a quantum on the order of 10^4 molecules of ACh. Upon excitation of the nerve endings, between 250 and 300 of these vesicles are released into the synapse, the controlled system. This corresponds to a release of approximately 10^{-17} moles of ACh. The transmission of the ACh is hindered by the action of the basal membrane, which secretes acetylcholinesterase. Thus the basal membrane is the controlling system, which exerts its influence through a rate of acetylcholinesterase activity. The membrane uses the ACh present at rest (which is effectively zero) as a reference signal u_r. Acetylcholinesterase is an enzyme that rapidly hydrolyzes ACh into acetic acid and choline, and is capable of destroying 10^{-14} moles of ACh within 5 msec. Therefore, the ACh released into the synapse (10^{-17} moles) is hydrolyzed in about 0.005 msec. The products of this breakdown are resynthesized inside the nerve terminals, and are available for the subsequent action potential.

Due to the almost instantaneous release of ACh upon excitation, we shall model this release as a spike function of amplitude 10^{-17} moles. We have assumed a pulse train of constant frequency, which is shown in Figure 13. If we denote the first impulse at $t = 0$ as $j = 0$, we can label each succeeding impulse as $j = 1, 2, 3, \ldots, f_s$. Note that an ACh release will occur for each impulse j, and will be hydrolyzed within a period of 5 μsec. If we denote the fractional portion of the time (i.e., real time minus the integer portion of the time) as t_f, it is possible to model the presence of ACh at time t in the form:

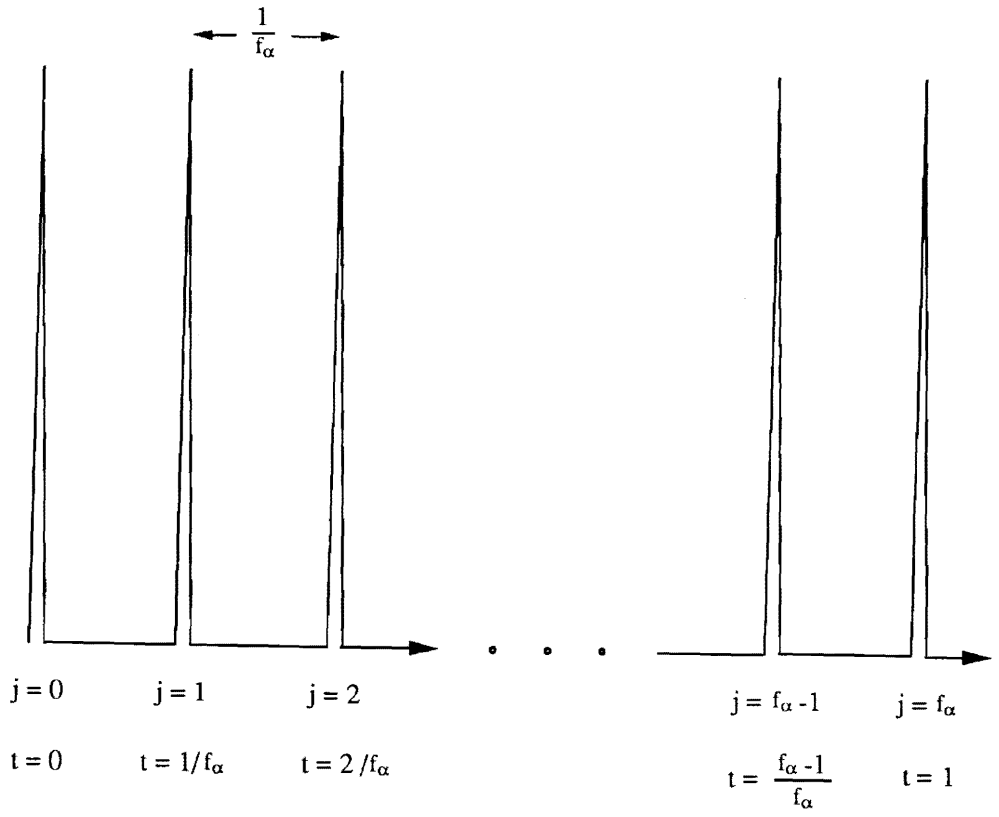

Figure 13. Alpha Motor-Neuron Impulse: The form of the pulse wave during the first second for a nervous impulse of frequency f_α. Each pulse is numbered from $j = 0$ to f_α, and time t_f is in seconds.

$$u(t) = \sum_{j=0}^{f_\alpha} 10^{-17} \exp(-1/\tau_s(t_f - j/f_\alpha)) \qquad [8]$$

where τ_s denotes the decay time constant of the signal. We can then describe the presence of ACh to be

$$ACh = \begin{cases} 0 \ for\ t_f < \dfrac{j}{f_\alpha} \\ u(t) \ for\ t_f \geq \dfrac{j}{f_\alpha} \end{cases} \qquad [9]$$

Since the acetylcholinesterase hydrolyzes the ACh in about 5 μsec, and the exponential decay function is within one percent of its limiting value (in this case zero) after five time constants, we can assume τ_s to be on the order of 1 μsec. This value measures the effectiveness of the control signal u_c, which is the rate of acetylcholinesterase hydrolysis.

Since the duration of the ACh spikes are so small, it is also possible to model their presence using the dirac delta function, $\delta(t)$. When its argument is equal to zero, this function describes an impulse of infinite amplitude and zero duration. It takes on a more meaningful value when employed under an integral sign, where limiting techniques can be utilized. In this case,

$$\int_0^t f(t)\delta(t - \frac{j}{f_\alpha})dt = f(\frac{j}{f_\alpha}) \qquad [10]$$

Using this relationship, and again using t_f as the fractional portion of the time, we can write

$$ACh = \sum_{j=0}^{f_\alpha} \int_0^t \hat{u}(t)\delta(t_f - \frac{j}{f_\alpha})dt \qquad [11]$$

where $\hat{u}(t) = 10^{-17}$ moles for all t.

The ACh that is released by the synaptic terminals is present for only a fraction of a second before it is hydrolyzed. In fact, for any accumulation of ACh above 10^{-17} to occur, the α-motor neuron must fire at frequencies exceeding 200,000 Hz. Since this never occurs in physiologic conditions, ACh summation is nonexistent in normally functioning synapses. The result is a series of ACh spikes, each generated by a separate nerve action potential. Thus, in normally functioning muscle, the frequency of the ACh spikes (f_{ACh}) impinging on the wall of the sarcolemma is equal to the frequency of stimulation (f_α), with a time delay due to the diffusion time in the synapse (which is on the order of 50 microseconds) (Schneck, 1991).

Thus our first control system, shown in Figure 12, consists of the basal membrane controlling the amount of ACh present in the controlled system, the synapse. The membrane "compares" the amount of ACh in the synapse, u_p, to the resting ACh, u_r. Due to the rapid hydrolysis rate of the acetylcholinesterase, this resting value is very nearly zero. The control signal u_c is the "activity" of the acetylcholinesterase, which can be represented as the time constant τ_s of equation [8]. The disturbing signal due to the α-motor neuron impulse is 10^{-17} moles per impulse. The amount of ACh at any given time can then be found using equation [9] or [11]. Due to the time course of the presence of ACh in "normal" synapses, the overall output u of the system can be given as the frequency of ACh spikes, f_{ACh}. This output now becomes the input u_d for the succeeding feedback control system, the propagation of the muscle action potential.

Transmission of the Muscle Action Potential

The ACh released is the disturbing signal for the subsequent controlled system, the sarcolemma (see Figure 14). The ACh molecules are thought to bond to protein receptors on the walls of the subneural clefts. The receptors activate the opening of pores of diameters ranging from 0.6 to 0.7 Angstroms, which allows a large number of sodium ions to permeate the sarcolemma. The rapid influx of sodium ions triggers a muscle action potential to propagate along the sarcolemma. As soon as the redistribution of ions occurs, the sodium-potassium pump (the controlling system) attempts to restore the equilibrium concentrations of the ions. The pump usually repolarizes the membrane within 5 msec, and the sarcolemma can then be depolarized by another nervous action potential. Due to the time required for repolarization, an f_α greater than 200 Hz will be unable to stimulate the sarcolemma, and the membrane is said to be in an absolute refractory state. The most active alpha-motor neuron seldom stimulates a muscle fiber faster than 100 times per second, thus each release of ACh should (and generally does) result in a corresponding muscle action potential. Thus the frequency of the end plate potentials $f_{\Delta Vep}$ should equal the frequency of the ACh spikes f_{ACh}, offset by a time delay. This characteristic time constant associated with the depolarization of the sarcolemma is on the order of 20 msec (Schneck, 1991).

The sarcolemma is a polarized membrane due to its selective permeability to specific ions and the presence within the membrane of various active ion pumps. Like other cell membranes, it is composed of a lipid bilayer with a large number of imbedded proteins. The lipid layer is responsible for the large capacitance of the membrane, which is approximately 1 μfarad (the lipid has a dielectric constant between 3 and 5). Measurement of the capacitance C_m has enabled calculation of the membrane thickness, which is between 7 and 10 nm. Due to the resting potential of the membrane (which is around -80 mV), the overall electrochemical gradient is on the order of 140,000 V/cm (Sperelakis and Fabiato, 1985). Potassium and sodium are the primary ions involved in the potential across the membrane,

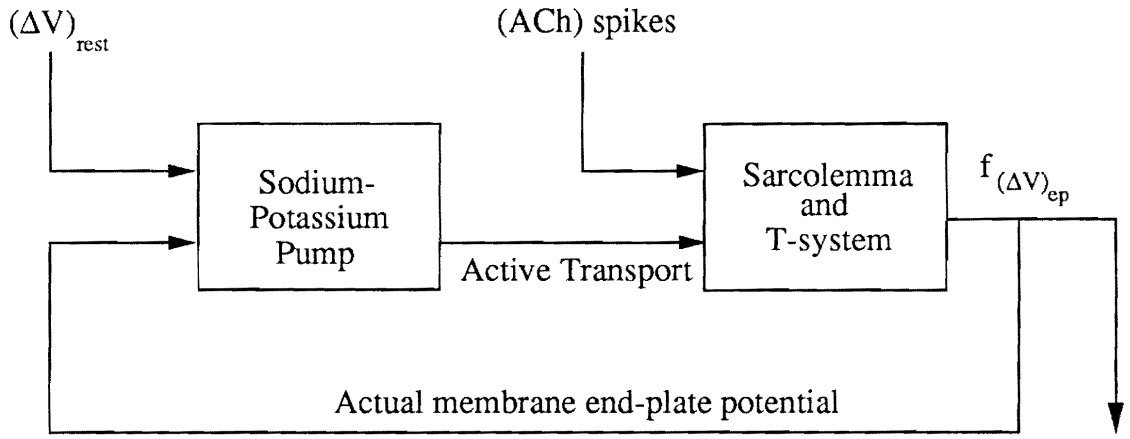

$$u_d = (ACh) \longrightarrow P_t = P_t(ACh)$$

$$u_r = -61 \ln \frac{P_{Na}[Na^+]_i + P_K[K^+]_i + P_{Cl}[Cl^-]_o}{P_{Na}[Na^+]_o + P_K[K^+]_o + P_{Cl}[Cl^-]_i}$$

$$u_c = \frac{\varepsilon[Y_m]AFZ}{\delta_m}$$

$$u: \quad \ddot{\beta} + c_4\dot{\beta} + c_5\beta = c_6 V_N \alpha(t)$$

Figure 14. Propagation of the Action Potential: The controlled system is the sarcolemma and T-system, the controlling system the sodium-potassium pump. $u_d = (ACh)$, u_r = -80 mV, u_c is given by equation [16], and u is given by equation [18] or expressed as the frequency of the action potential.

with calcium and chlorine playing lesser roles. The resting concentrations which are present on either side of the membrane, as well as the major active transport mechanisms of the membrane, are shown in Figure 15.

These concentrations establish an equilibrium potential E_n for each of the ions. This value denotes the electrical force which opposes (and exactly balances) the concentration gradient of the ions. The equilibrium potential is calculated using the Nernst equation, which at 37 degrees Celsius is:

$$E_n = \frac{-61}{Z} \log \frac{C_i}{C_o} \qquad [12]$$

C_i and C_o are the concentrations of the ion inside the cell and outside the cell, respectively. Z is the valence of the ion, sign included, and each E_n is given in mV. The driving force for the ion is the difference between the resting potential and the equilibrium potential, $E_m - E_n$. The driving forces for the four ions are: $E^{Na}{}_f = -140$ mV, $E^{Ca}{}_f = -209$ mV, $E^{Cl}{}_f = 0$ mV and $E^{K}{}_f = +14$ mV. A negative $E^{n}{}_f$ denotes a driving force into the cell. Each driving force will play a major role in the establishment of an action potential, and thus will affect our transfer function for the control system in Figure 14.

The resting potential E_m (which is the u_r for the control system) can be found by using the Goldman Equation (Schneck, 1991 and Guyton, 1986).

$$E_m = \frac{RT}{FZ} \ln\left(\frac{P_K[K^+]_o + P_{Na}[Na^+]_o + P_{Cl}[Cl^-]_i}{P_K[K^+]_i + P_{Na}[Na^+]_i + P_{Cl}[Cl^-]_o} \right) \qquad [13]$$

where R is the universal gas constant 8.31 $J\,mole^{-1}K^{-1}$, F is Faraday's constant 96500 $coulombs\,mole^{-1}$, T is the absolute temperature 310 K, and Z is the valence of the ion being moved, which is unity for each of the ions above. The subscript i denotes inside the cell, o is outside the cell. Note that the chlorine ion has a valence of -1; negative ions inside the cell

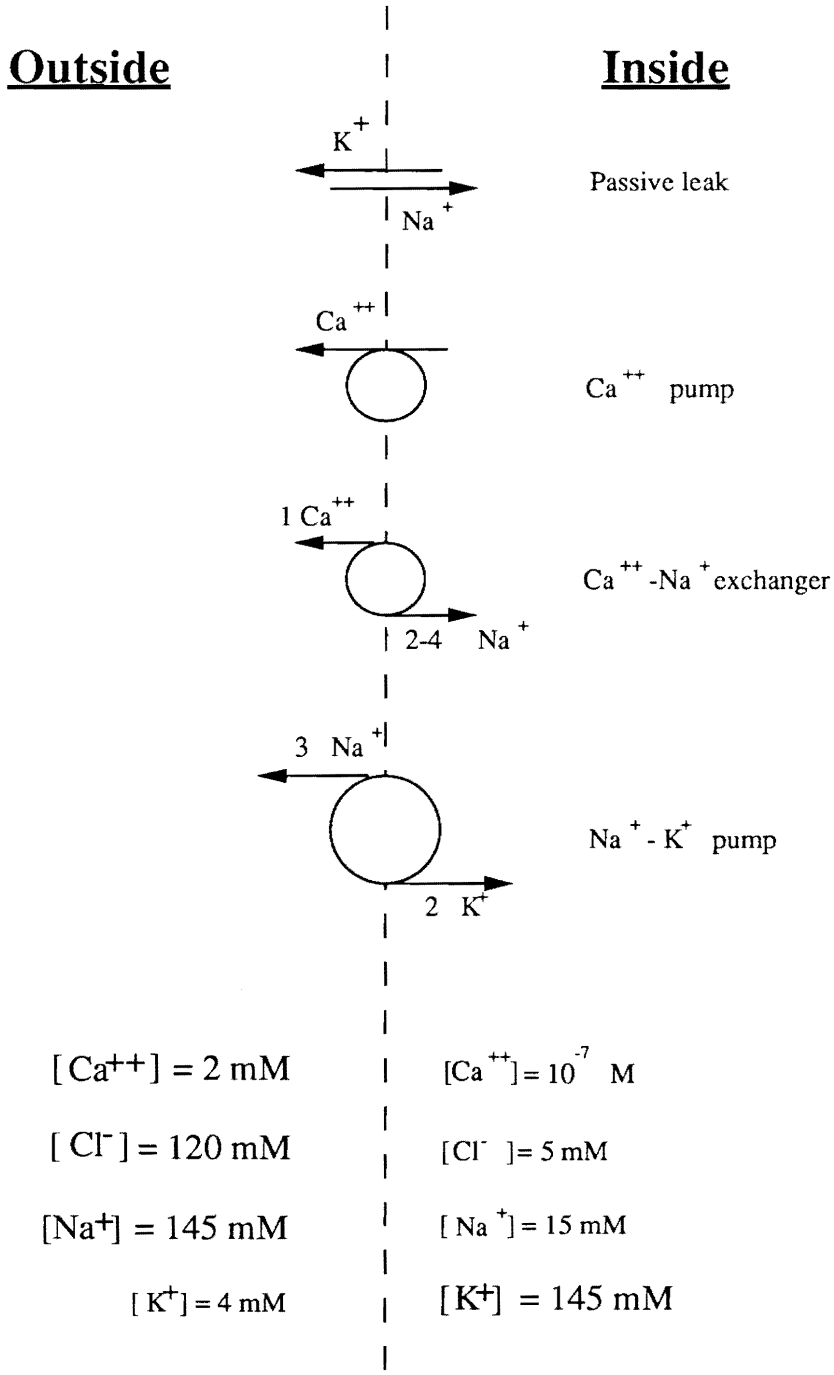

Figure 15. Resting Concentrations Across the Sarcolemma: The concentrations of the major ions involved in the action potential, and the various active mechanisms present in the membrane.

contribute the same potential as a positive ion outside the cell. Each P_n denotes the permeability of the membrane to each ion, n. Sperelakis and Fabiato (1985) offer an alternate method of calculating the resting potential E_m using the chord-conductance equation:

$$E_m = \frac{g_K}{g_K + g_{Na}} E_K + \frac{g_{Na}}{g_K + g_{Na}} E_{Na} \qquad [14]$$

In this equation the contributions of Cl^- and Ca^{++} are deemed negligible. The conductance of the ions is denoted by g_n and is measured in Ω^{-1}. Conductance is the reciprocal of the resistance through which the ions must travel, and is thus controlled by the permeability of the membrane to each specific ion. Equations [13] and [14] yield a resting potential u_r between -60 and -90 mV, inside negative relative to outside.

The driving force calculated in equation [12] is responsible for the flow of ions across the membrane. Ohm's law, $V = IR$ can be modified to obtain the expression:

$$I_n = g_n(E_m - E_n) \qquad [15]$$

for each ion, n. Once again, g_n is the conductance of the ion through the membrane. It is changes in the value of this conductance which allow the action potential to propagate.

The disturbing signal u_d to the sarcolemma is caused by the release of ACh into the synapse. The ACh molecules bond to receptor-activated proteins in the cell wall. These proteins change conformation, opening up pores of 60 to 70 nm and increasing the permeability of the membrane by some thousand fold. This increases g_{Na} considerably, and using equation [15] for sodium, ($I_{Na} = g_{Na}E_{Na}'$), we see that I_{Na} will increase considerably. An initial rapid influx of sodium ions will reduce the potential difference by approximately 20 mV. At levels between -70 and -50 mV, a voltage-regulated fast sodium channel is activated. This "gate" increases g_{Na} even more (the permeability of the membrane to sodium increases some 500-5000 fold), and an extremely rapid influx of Na^+ results. The potential difference across

the membrane increases at a rate of 400-700 V/sec over a period of about one msec. After this initial increase, the voltage-regulated sodium channel turns off and a slow, voltage-regulated potassium channel is activated. The efflux of K^+ reduces the potential difference of the membrane, and brings the sarcolemma back down towards its resting potential (Guyton, 1986).

In order to restore the equilibrium potentials and the driving forces which existed before the action potential, the $Na^+ - K^+$ pump becomes extremely active. The pump rate is a function of external K^+ and actually exhibits a cubic dependence on internal Na^+. The activity of this pump, which is the controlling signal u_c for the system of Figure 14, can be measured by the rate at which the sodium ions are pumped out of the sarcoplasm. This can be approximated by the equation:

$$(u_c)_{max} = \frac{\varepsilon[Y_m]AFZ}{\delta_m} \qquad [16]$$

This equation describes the activity of the carrier protein involved in the pump, where ε is the dissociation constant in sec^{-1} between sodium and the carrier molecule Y and $[Y_m]$ is the maximum molar concentration of Y in the membrane. A is the transport area, δ_m is the thickness of the membrane, F is the Faraday constant, and Z is the valence.

The action potential generated by the ACh receptors then activates adjacent voltage-regulated channels, and the action potential propagates along the length of the sarcolemma. Sperelakis and Fabiato (1985) calculate the velocity of propagation v_{ap} to be dependent on the fiber radius a, the membrane capacitance, C_m, the membrane resistance, and the resistivity of the sarcoplasm:

$$v_{ap} = \sqrt{\frac{a}{2R_m R_i C_m}} \qquad [17]$$

where R_m is the membrane resistance normalized for fiber radius and length and and R_i is the sarcoplasmic resistivity normalized for length and cross-sectional area. Using equation [17] the action potential generally propagates at a velocity of about 5 m/sec. Once the action potential reaches the T-tubules, it propagates to the interior of the cell with a velocity of about 10 cm/sec. The resulting T-system action potential, or more specifically the frequency of this action potential, is the output u of Figure 14.

Hatze (1981) describes the propagation of the action potential using a lumped second-order system, where the signal along the sarcolemma and the T-system is combined. This potential is modelled as:

$$\ddot{\beta} + c_4\dot{\beta} + c_5\beta = c_6 V_N \alpha(t) \qquad [18]$$

with boundary conditions $\beta(0) = \dot{\beta}(0) = 0$. The impulse of the alpha-motor neuron, V_N is the driving function of the membrane depolarization, and c_4, c_5 and c_6 are constants calculated from empirical data. Such an analysis could easily be applied to the control system of the propagation of the muscle action potential.

Thus the ACh begins a change of events which is controlled by the repolarizing effects of the $Na^+ - K^+$ pump. The u_d causes a change in permeability P_t, which is normally 3 to 4 times greater than that needed to stimulate an action potential. The controlling signal for this system is the activity of $Na^+ - K^+$ pump, which is quantified in equation [16]. The reference signal is found by equations [13] or [14]. Finally, the output u, which is the depolarization of the membrane, can be found using equation [18].

Similarly to the ACh impulses, the action potential should propagate at the same frequency as f_α. This frequency $f_{\Delta Vep}$ can also be used as the output u of the control system. The action potential propagates along the sarcolemma at a speed of 5 m/sec, then decreases to about 10 cm/sec through the T-tubules. This action potential serves two main functions. The first is to hydrolyze water in the sarcoplasm, which is necessary to maintain the energy resources of the muscle cell. This function will be discussed at length later. The second event

caused by the muscle action potential involves the release of Ca^{++} into the sarcoplasm, which is discussed below.

Release of Calcium

As the muscle action potential propagates along the transverse tubules, it reaches an area known as the triad. This is a junction where the tubules come into close contact with the sarcoplasmic reticulum, a membranous structure which is present throughout the muscle cell. Attached to this membrane are small cisterns, which contain large amounts of Ca^{++}. Gillis et al. (1982) report the amount of Ca^{++} which can be readily released from the cisterns to be on the order of 700 μmolar. Each action potential in the tubules somehow induces these cisterns to release some of these calcium ions into the sarcoplasm. It is thought that a voltage-regulated movement of proteins within the transverse tubule membrane opens up pores within the sarcoplasmic reticulum cisterns (see Sperelakis and Fabiato, 1985 and Rios and Pizarro, 1988). The greater the number of impulses, the larger the number of pores opened. Higher frequencies will increase the duration that these pores are open. Thus, the frequency of the action potentials $f_{\Delta Vep}$ is the disturbing signal, which controls the amount of Ca^{++} released by the controlled system, the sarcoplasmic reticulum cisterns.

As soon as the Ca^{++} is released into the sarcoplasm, it activates a pumping mechanism which begins to sequester the ions back into the sarcoplasmic reticulum cisterns. The calcium pump (the controlling system) "compares" the amount of Ca^{++} present to a reference signal, the amount of ions present in the sarcoplasm when the muscle is at rest. If the concentration is greater than this $[Ca^{++}]_{rest}$ (which is generally about 10^{-9} molar), then the calcium pump will begin to remove the ions from the sarcoplasm by an active transport mechanism, the control signal. The entire control system of Ca^{++} concentration in the sarcoplasm is shown in Figure 16.

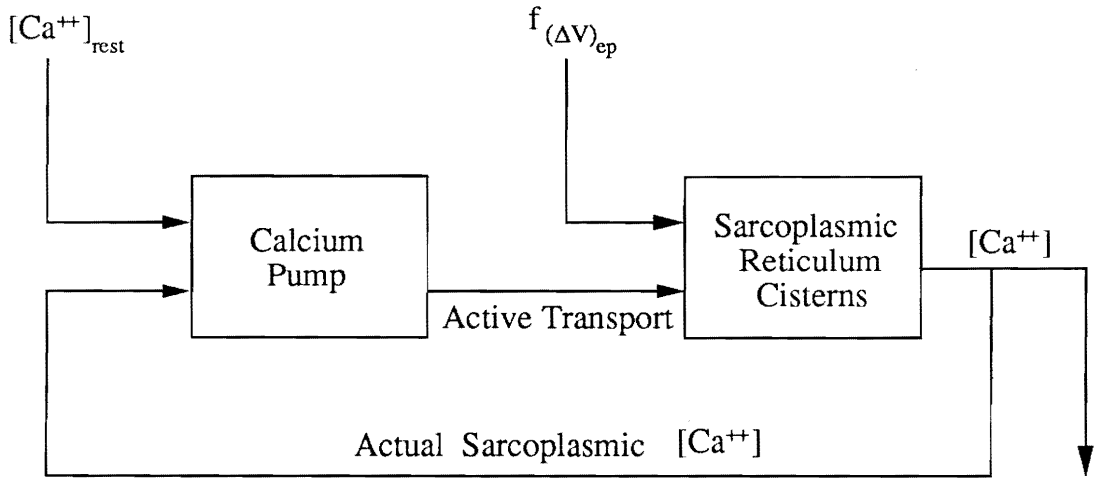

$$u_d = V_{ep}$$

$$u_r = [Ca^{++}]_r = 10^{-9}\ M$$

$$u_c = \frac{dCa}{dt} = \frac{V_{max} + [Ca^{++}]}{[Ca^{++}] + K_m}$$

$$u : \ddot{\gamma} + \frac{c_1\dot{\gamma} + c_2\gamma}{\rho(x)} = c_3 V_T \beta(t)$$

or

$$[Ca^{++}](f_\alpha, t) = [Ca^{++}](f_\alpha)\,[Ca^{++}](t)$$

Figure 16. Release of Calcium Ions: The controlled system is the sarcoplasmic reticulum cisterns, the controlling system the calcium pump. u_d is $f_{\Delta V ep}$, $u_r = 10^{-9}$ M Ca^{++}, u_c is given by [24], and u is given by [25] or [26].

The rate of this active transport will determine how quickly the Ca^{++} is resequestered into the sarcoplasmic reticulum, while the frequency of the action potential $f_{\Delta Vep}$ will determine how quickly the sequestered ions are released. If the frequency of stimulation is too large for the pump to handle, Ca^{++} summation will occur, and larger and larger amounts of calcium will accumulate in the sarcoplasm. If the concentration of these ions reaches a threshold of approximately 6×10^{-7} molar (which corresponds to a $f_{\Delta Vep}$ of approximately 4 Hz), the calcium causes a subsequent chain of events in the muscle tissue which results in a contraction. If the stimulation occurs at an sufficiently rapid rate, the cisterns release the Ca^{++} almost instantaneously (like pouring water into a bucket with a hole in the bottom). All of the available Ca^{++} will then be present in the sarcoplasm. This results in tetanus, which corresponds to a $[Ca^{++}]$ of about 2×10^{-4} molar and a $f_{\Delta Vep}$ of about 100 Hz for fast-twitch muscle and 40 Hz for slow-twitch muscle.

Many researchers have developed calcium compartmental models in an attempt to explain Ca^{++} kinetics in the myoplasm. A familiar approach is to use exponential functions multiplied by an amplitude factor to determine Ca^{++} concentrations. Gillis et al. (1982) determine calcium release to be a function of time where:

$$(Ca^{++}entry)_t = [Ca^{++}]_{sp}(1 - Ae^{-t/\alpha} + Be^{-t/\beta}) \qquad [19]$$

A and B are amplitude factors, while α and β are fall and rise time constants, respectively. $[Ca^{++}]_{sp}$ is the calcium concentration released by a single action potential. The investigators use the following values for the equation: A= 1.1525, B= 0.1525 (both dimensionless), α = 6.0 msec, β = 0.8 msec, and $[Ca^{++}]_{sp} = 200\ \mu$molar Ca^{++} per liter of muscle. Robertson et al (1981) calculate the pCa(t), where $pCa = -\log_{10}[Ca^{++}]$ to be:

$$pCa(t) = pCa_{relax} - A(e^{-t/f} - e^{-t/r}) \qquad [20]$$

pCa_{relax} denotes the resting pCa, which was taken to be 8 (which corresponds to $[Ca^{++}] = 10^{-8}$ molar). A is given as 3.26, r as 0.5 msec, and f as 15 msec. In a third investigation, Cannell and Allen (1984) calculate the changing permeability of the sarcoplasmic reticulum. This permeability is in reality a velocity measurement, indicating the speed with which the Ca^{++} molecules diffuse across the membrane.

$$P_t = P_{max}[1 - \exp(-t/\tau_{on})][\exp(-t/\tau_{off})] \qquad [21]$$

P_{max} is the maximum permeability of the wall, which is 0.062 mm/sec. The signal is presumed to turn "on and off" exponentially, with time constants $\tau_{on} = 1$ msec and $\tau_{off} = 5$ msec.

We shall assume that the calcium release is simply a function of the frequency of the action potential, which is the same as the frequency of stimulation f_α. This assumption presupposes that the release of calcium is nearly instantaneous, and can be represented as a step function. Therefore we can determine $[Ca^{++}]$ as a function of $f_{\Delta Vep}$ by finding a curve-fit to experimental data. Such experiments are well-documented, most notably the work of Bendall (1969). The response of Ca^{++} to a frequency of stimulation is in the shape of an S-curve, which can be approximated using the Hill Equation:

$$\Gamma = \frac{\left(\frac{p}{p_o}\right)^n}{1 + \left(\frac{p}{p_o}\right)^n} \qquad [22]$$

We will set

$$\frac{[Ca^{++}] - [Ca^{++}]_o}{[Ca^{++}]_\infty} = \frac{\left(\frac{f_\alpha}{f_{0.5}}\right)^n}{1 + \left(\frac{f_\alpha}{f_{0.5}}\right)^n} \qquad [23]$$

$[Ca^{++}]_o$ is the concentration of calcium at rest, $[Ca^{++}]_\infty$ is the concentration at tetanus, and $[Ca^{++}]$ is the concentration of calcium present in the sarcolemma due to a certain frequency of stimulation. The variable $f_{0.5}$ is the frequency of stimulation which corresponds to a calcium concentration equal to half of its maximal value. The exponent n can be determined by applying certain boundary conditions. If we use:

$f_\alpha = 4$ Hz when $[Ca^{++}] = 6 \times 10^{-7}$ M (threshold)

$f_{0.5} = 50$ Hz when $[Ca^{++}] = 1 \times 10^{-4}$ M

$f_\alpha = 100$ Hz when $[Ca^{++}] = 2 \times 10^{-4}$ M (tetanus)

we obtain an exponent n equal to 2.4 . Equation [23] can now be used to determine the calcium ion release as a function of any given frequency.

The kinetics of the calcium pump have also been modelled. The most common analytical technique to describe the pump mechanism is to utilize Michaelis-Menten kinetics. A derivation of the method can be found in Schneck (1990). The pump rate is described by:

$$\frac{dCa}{dt} = \frac{V_{max}[Ca^{++}]_{ems}}{[Ca^{++}]_{ems} + K_m} \qquad [24]$$

where $[Ca^{++}]_{ems}$ is the free calcium concentration in the extramyofibrillar space, V_{max} is the maximum pump rate, and K_m is the calcium concentration at one-half the maximal pump rate. Cannell and Allen (1984) use values of $K_m = 10^{-6}$ molar and $V_{max} = 1$ mmolar/sec, while Gillis et al. (1982) arrive at values of $K_m = 10^{-7}$ molar and $V_{max} = 0.7$ mmolar/sec.

Hatze (1981) performs an analysis similar to that of equation [18]. In this case the propagation of the action potential β multiplied by the average depolarization of the membrane (about 0.05 V) is the forcing function. The overall calcium response is denoted by γ, and the free filamentary calcium concentration is given by:

$$\ddot{\gamma} + \frac{(c_1\dot{\gamma} + c_2\gamma)}{\rho(\xi)} = c_3 V_T \beta(t) \qquad [25]$$

He calculates a normalized calcium density function $\rho(\xi)$ which is a function of a normalized contractile element length ξ. Each c_i is a constant found from experimental data.

Another approach to modelling the decay of the myofibrillar concentration due to the calcium pump is similar to the method applied to the ACh control system. An amount of Ca^{++} will be released which is proportional to the frequency of stimulation. This will decrease during each time interval when the actual depolarization is not impinging upon the triad. This can be modelled using a separation of variables approach where calcium ion concentration is the product of a function of f_α and a function of time:

$$[Ca^{++}](f_\alpha, t) = [Ca^{++}](f_\alpha)[Ca^{++}](t) \qquad [26]$$

$[Ca^{++}](f_\alpha)$ is given by equation [23], while $[Ca^{++}](t)$ indicates the action of the calcium pump. It can be modelled similarly to equation [8], where again t_f is the factional portion of time in seconds, and we assume an exponential decay. $[Ca^{++}](t)$ may also be a solution to equation [24], which describes the pump rate. Either form may be used in equation [26] in order to model the concentration of calcium ions in the sarcoplasm, which is the output u of the control system in Figure 16.

This control system is initially disturbed by a u_d which is the muscle action potential. The control signal u_c is expressed as the activity of the Ca^{++} pump, which is given by equation [24]. The output due to these signals is the amount of Ca^{++} present in the myoplasm, which is given by equations [25] or [26]. The output may also be obtained by coupling the calcium release (given by equations [19], [20], and [21] to the calcium uptake (given by equation [24]. This u is the disturbing signal for two subsequent control systems, each involving regulatory mechanisms.

Thin Filament Regulation

The calcium ions that are released into the myoplasm are utilized in a variety of ways. Many are resequestered into the sarcoplasmic reticulum cisterns, as described above. There are a number of calcium ion buffers, most notably the protein parvalbumin, which can bind the myoplasmic calcium. Some ions are thought to bind to the myosin head, which plays a role in thick filament regulation. Finally, the most important receptor of calcium is the regulatory binding sites on the troponin-C (TnC) molecules.

Each TnC molecule possesses four binding sites. Two high-affinity sites (binding constant of $K = 10^{-8}$ M) bind both calcium and magnesium, and do not seem to play a role in regulation. The two low-affinity sites ($K = 10^{-6}$ M), however, are calcium specific and do exert a regulatory role on the muscle (Cannell and Allen, 1984 and Gillis et al., 1982). The TnC exerts an influence on tropomyosin, which is in close contact with the actin molecule. The tropomyosin undergoes some type of configurational change, which uncovers a site on the actin molecule to which the myosin can bind. Due to X-ray diffraction data, it is thought that the tropomyosin molecule actually "moves" into the grooves between the actin filaments, allowing a myosin head to bind to the actin. This mechanism is known as the steric blocking model, and is shown schematically in Figure 7.

This mechanism, which is the controlled system, is often referred to as the protein switch of muscle contraction. The Ca^{++} present in the sarcoplasm is quickly resequestered by the calcium pump, the controlling system. Due to lower concentrations in the sarcoplasm, a concentration gradient between the TnC low-affinity sites and the sarcoplasm is established. This exerts a dissociation effect (which is the control signal for the system) on the protein switch and reduces the number of available actin binding sites. The reference signal u_r is the $[Ca^{++}]$ at rest and the primary feedback signal is the amount of TnC sites not bound to calcium ions. The control system is shown in Figure 17.

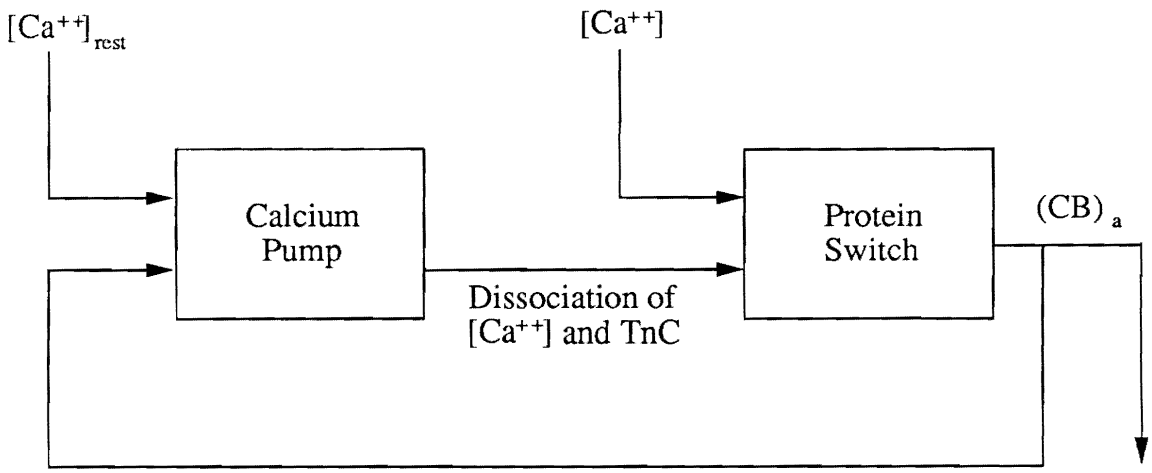

$$u_d = [Ca^{++}]$$

$$u_r = 10^{-9} M$$

$$u_c = K_{off}$$

u:

$$\frac{d[Ca^{++}TnC]}{dt} = K_{on}[Ca^{++}][TnC] - K_{off}[Ca^{++}TnC]$$

Figure 17. Thin Filament Regulation: The controlled system is the protein switch, the controlling system the calcium pump. u_d is the concentration of calcium ions in the sarcoplasm, $u_r = 10^{-9}$ M of Ca^{++}, u_c is expressed by the dissociation rate K_{off}, and u is related to equation [27].

Several authors (Mezler, 1984; Cannell and Allen, 1984; Gillis et al, 1982) have again used Michaelis-Menten kinetics to describe the binding of Ca^{++} to the regulatory sites of the TnC. The net flux of TnC sites absorbing calcium ions is given by:

$$\frac{d[Ca^{++}TnC]}{dt} = K_{on}[Ca^{++}][TnC] - K_{off}[Ca^{++}TnC] \qquad [27]$$

where K_{on} and K_{off} are association and dissociation constants, respectively. The rate constants and concentration of TnC binding sites used by three different studies is given in Table 2.

Thus the control system of Figure 17 is disturbed by the release of Ca^{++} calculated in equations [25] or [26]. This causes a certain number of TnC sites to become "activated", as evident by the term $K_{on}[Ca^{++}][TnC]$ in equation [27]. The reference signal for the calcium pump is the resting Ca^{++} which is about 10^{-9} M. The control signal is a function of the concentration gradient present between the sarcoplasm and the TnC sites, expressed in equation [27]. The output u is also described by this equation and is related to the number of TnC-Ca^{++} complexes formed. Each TnC molecule that has Ca^{++} bound to it affects seven actin monomers. Thus the number of actin binding sites is a direct product of the amount of TnC - Ca^{++} complexes, and the output $(CB)_a$ of the system in Figure 17 can be found by using the solution to equation [27].

The Energy Loop

The calcium ions are originally activated by the muscle action potential which propagates along the T-system. This potential not only initiates the release of calcium ions from the sarcoplasmic reticulum cisterns, but also serves to hydrolyze the water molecules (the controlled system) present in the sarcoplasm. The mitochondria is the controlling system over

Table 2. Binding Constants of TnC and Calcium Ions

K_{on} ($M^{-1}sec^{-1}$)	K_{off} (sec^{-1})	Tn ($x\ 10^{-6}$ M)
0.575×10^{-8}	115	240 (a)
1.20×10^{-8}	120	140 (b)
1.0×10^{-8}	31.6	140 (c)

(a) Mezler et al. (1984)
(b) Cannell and Allen (1984)
(c) Gillis et al. (1982)

the water present in the energy cycle, and exerts its influence through the numerous Krebs cycle enzymes. The reference signal for the mitochondria is the amount of products present during rest. The mitochondria not only controls the activation of the Krebs cycle, but also the hydrolysis of ATP. The control signal is a product of the many Krebs cycle enzymes which catalyze the splitting of ATP. The disturbing signal is actually the output H^+ of the previous controlled system, the water of the energy cycle. The output of the ATP hydrolysis depends on a number of circumstances, which are described below. The processes involved in the production of energy are shown in Figure 18, and described in greater detail elsewhere (e.g. Schneck, 1991 and Guyton, 1981).

Normally, the ATP molecule splits to form adenosine diphosphate (ADP) and phosphoric acid in an exergonic reaction. The energy released in this reaction is approximately 7600-7800 calories per mole of ATP hydrolyzed. This corresponds to a maximum energy release of 800 cal/min per kg of body weight. If, however, lactic acid accumulates to a high enough level, the breakdown of ATP is blocked. The toxicity level of lactic acid is reached when the energy requirements from the breakdown of the fructose diphosphate reaches 2600 cal/min per kg of body weight.

The phosphoric acid formed in a normal reaction then reacts with glucose present in the cell (glucose can also be formed from glycogen which is stored in the muscle tissue). The product, fructose diphosphate, then reacts in one of two ways. If there is sufficient oxygen present in the sarcoplasm (aerobic metabolism), the fructose diphosphate is oxidized into phosphoric acid, carbon dioxide, and water. This is an exergonic reaction which produces 670,000 calories per mole of glucose oxidized. If there is not enough oxygen present (anaerobic metabolism), the fructose diphosphate breaks down into lactic acid and phosphoric acid, releasing 230 calories per gram of lactic acid produced. It is this lactic acid that can accumulate in the sarcoplasm and block the breakdown of ATP.

The phosphoric acid produced by the breakdown of fructose diphosphate combines with creatine present in the muscle tissue to form phosphocreatine. This compound readily breaks down into phosphoric acid and creatine, releasing some 220 cal/min per kg of body weight.

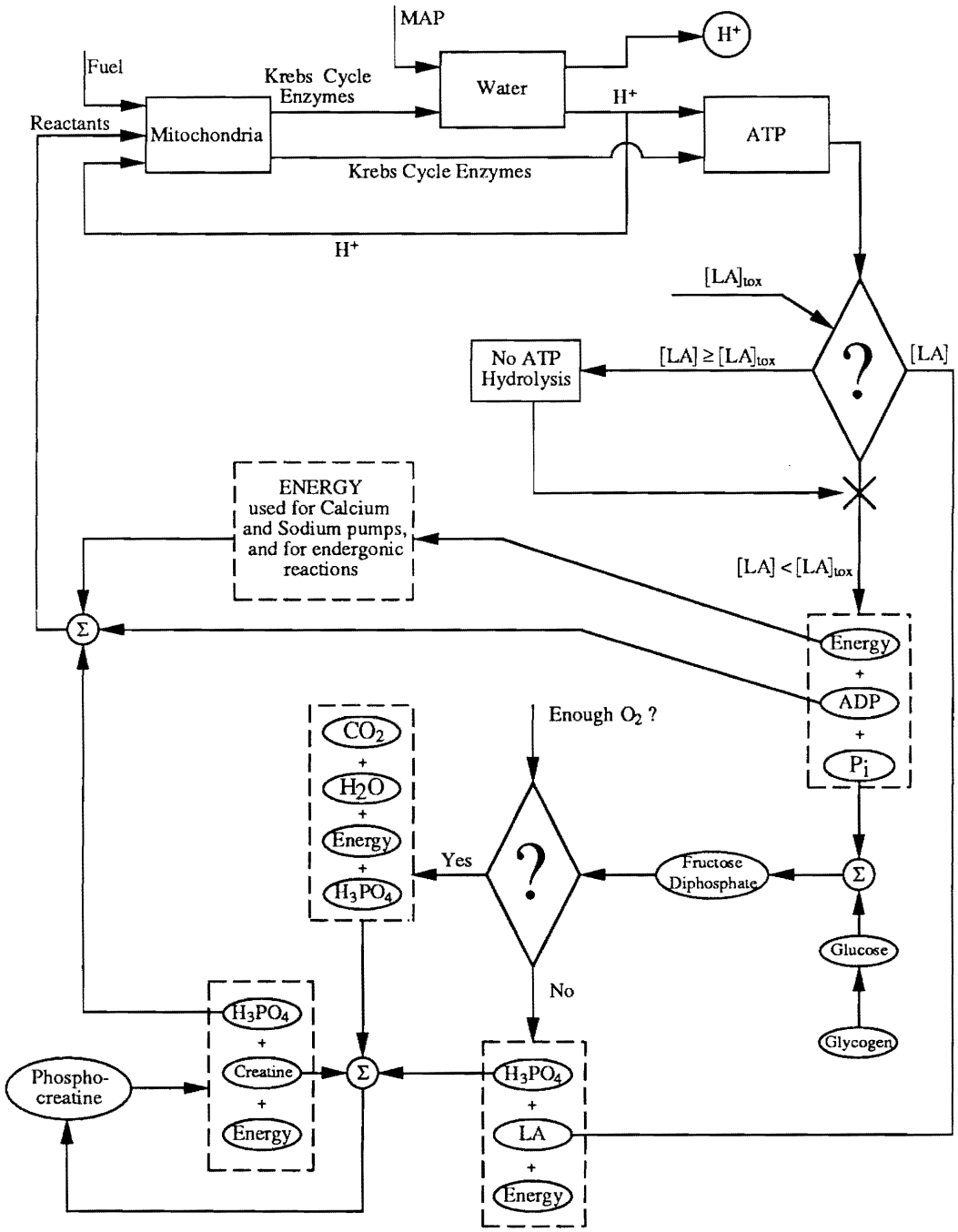

Figure 18. The Energy Loop: The mechanisms of energy production are shown.

This phosphoric acid then combines with the ADP produced in the original breakdown of the ATP. In a process known as the Lohman reaction, the ADP and the phosphoric acid combine in an endergonic reaction to form a new molecule of ATP. Thus the energy cell is refueled, ready to begin another cycle.

The kinetics of the numerous biochemical reactions taking place are complex. Needless to say, it is beyond the scope of the present work to try to quantify the reaction rates and various metabolic concentrations. We shall assume that the input to the system, the muscle action potential, hydrolyzes water that begins the processes of energy loop. The output of this loop, u of Figure 18, consists of hydrogen ions, energy for the various endergonic processes in the sarcoplasm, and the products of the ATP hydrolysis.

Thick Filament Regulation

The hydrogen ions from the energy loop then act in concert with the calcium ions to disturb the myosin head. This causes a hydrolysis of the myosin-bound ATP, which yields an output u of $(CB)_m$, dissociation products, and energy. The active $(CB)_m$ sites are then controlled by the Lohman reaction, which is the controlling system. This reaction is thought to resynthesize an ATP molecule on the myosin head, which exerts a dissociation effect on the actomyosin complex. The reaction is "fueled" by the dissociation products of the ATP (i.e., ADP and P_i) from both the energy loop and the thick filament regulatory mechanism. The control system is shown in Figure 19.

Although regulation of muscle contraction in vertebrates primarily involves the thin filaments, several lower organisms exhibit thick filament regulation. Molluscan muscle, which contains negligible amounts of troponin, nevertheless exhibits ATPase rates which are regulated by calcium. It was found that a specific light chain, generally referred to as the DNTB regulatory light chain or LC_2, was responsible for this calcium sensitivity (see Bagshaw, 1982). In a recent study performed by Hofmann et al. (1990), LC_2 is removed from skinned rabbit

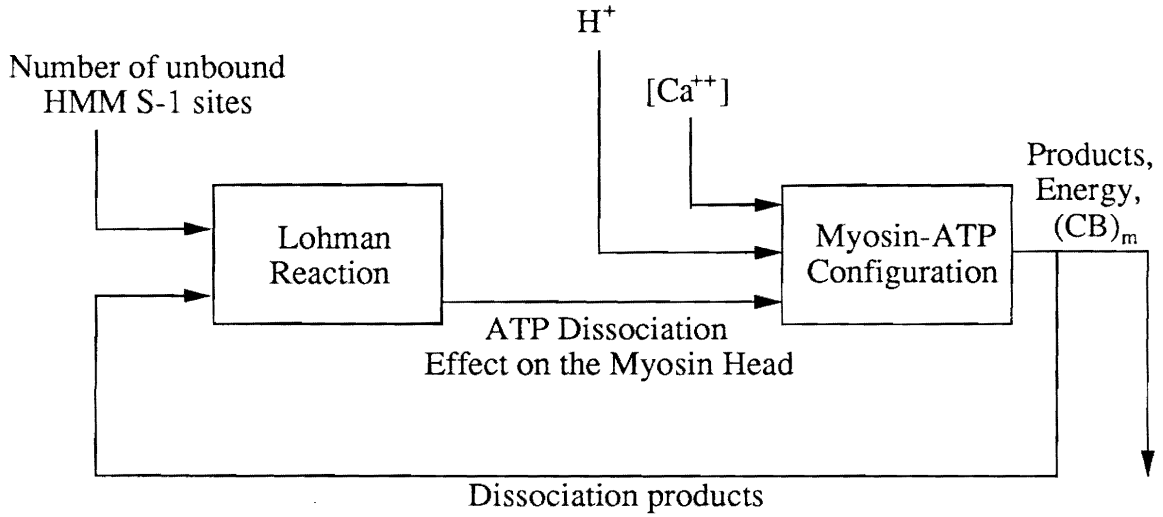

$$u_d = [Ca^{++}] \qquad u_d = [H^+]$$

$$u_c = K_{off}$$

$$u_r = \text{all HMM S-1 sites}$$

$$u = 3800 \text{ calories/mole ATP}$$

and

$$\frac{d[Ca^{++}LC_2]}{dt} = K_{on}[Ca^{++}][LC_2] - K_{off}[Ca^{++}LC_2]$$

Figure 19. Thick-Filament Regulation: The controlled system is the HMM S-1 of the myosin head, the controlling system the Lohman reaction. u_d is a combination of hydrogen and calcium ions, u_r is the number of unbound HMM S-1 sites at rest, u_c is the dissociation effect of the ATP on the cross-bridge, and u is $(CB)_m$, energy, and the dissociation products.

psoas fibers. Removing partial amounts of the light chain and subsequently reintroducing them affects the velocity of contraction as well as the tensions developed. The effects at different calcium levels are also studied. The authors conclude that the LC_2 most probably affects the region of the S1-S2 hinge, through a calcium-induced conformational change. They further suggest that the LC_2 may control the rate of cross-bridge detachment during shortening, as well as the number of cross-bridges formed.

Using this as a possible mechanism of thick filament regulation, we postulate the following sequence of events to occur. The hydrogen atom hydrolyzed by the muscle action potential not only attacks the ATP present in the sarcoplasm, but also combines with the calcium ions to alter the configuration of the myosin head (which contains a bound ATP molecule). According to some theories (Hatze, 1973), the Ca^{++} binds to the top of the HMM S-1, changing the electrostatic charge on the myosin head. The resulting configurational change brings the HMM S-1 bound ATP molecule into closer proximity to the ATPase region of the HMM S-2 subfragment. This, along with the hydrolyzing action of the hydrogen ions present, causes breakdown of the ATP molecule.

Thus, the Ca^{++} and the H^{+} (the u_d's) disturb the myosin-ATP configuration (the controlled system). This results in a hydrolysis of the ATP, which releases ADP and phosphoric acid in an energy producing reaction (see previous description of the energy loop). This also exposes a site on the HMM S-1 myosin head which can now freely bond to the actin molecule. Therefore the output u of the system is a combination of $(CB)_m$, the hydrolysis products, and energy. The total useable energy due to the hydrolysis of one mole of ATP is around 3700 calories (assuming 50 percent efficiency). When the ATP molecule is released, the Lohman reaction (the controlling system) attempts to resynthesize a new ATP molecule on the myosin head. When this occurs, the ATP exerts a dissociation effect u_c on the actin-myosin complex and the HMM S-1 binding site is no longer free to bond to the actin. The control system of thick-filament regulation is shown in Figure 19.

The binding of the Ca^{++} to the LC_2 can be described using Michaelis-Menton kinetics, as in equation [27]:

$$\frac{d[Ca^{++}LC_2]}{dt} = K_{on}[Ca^{++}][LC_2] - K_{off}[Ca^{++}LC_2] \qquad [28]$$

The rate constants for these binding processes have not been determined.

The effect of the hydrogen ions on the hydrolysis of the ATP molecule on the myosin head involves the kinetics of the ATP hydrolysis cycle. Unfortunately little research has been done on thick-filament regulation in mammalian skeletal muscle, but perhaps the recent findings of Hofmann et al. (1990) will stimulate further work in the field. This loop does, however, make our control model applicable to other types of muscle such as that of the mollusk. In this case the thin-filament regulatory loop would contribute relatively little to the overall formation of cross-bridges, while the thick-filament loop would prove to be dominant. By changing the various transfer functions to represent the mechanisms of the contractile process, it is possible to model nearly all types of muscle contractions, and obtain an appropriate output CB_m for the control system.

Number of Cross-Bridges Formed

As shown in Figure 11, the total number of cross-bridges formed is a function of the number of available actin binding sites $(CB)_a$, together with the number of available myosin binding sites $(CB)_m$ with which they can be paired. Secondly, the extent of filamentary overlap of the sarcomere, as well as the speed with which the filaments slide past one another, have been found to be important in the formation of a cross-bridge. We have assumed that the thick and thin filament regulatory mechanisms are separate, when in fact they are intricately connected. The ATPase rate of the myosin head is extremely actin-sensitive. The available Ca^{++} must compete with magnesium for the various regulatory sites present. There is most likely a series of complex control mechanisms which regulate the formation of the cross-

bridges. For simplicity, we have utilized a separation of variables approach to describe the regulation of muscle contraction.

The number of cross-bridges formed, CB, depends on the degree of filamentary overlap, in the sense that the HMM S-1 heads will have no opportunity to establish cross-bridges if there are no actin sites nearby (i.e. a stretched sarcomere). Likewise, if there are too many myosin heads in a single location, they will have to compete for the available actin binding sites. The contraction speed will also affect cross-bridge formation, due to the fact that thin filaments which are sliding rapidly past the myosin heads limit the opportunity to establish cross-bridges. One way to account for these two factors (filamentary overlap and contraction speed) is to include a feedback loop from the overall response, δ and $\dot{\delta}$, of the muscle fiber (see Figure 11). The transfer function for the total number of cross-bridges formed is given by:

$$CB = CB\{CB_m, CB_a, \delta, \dot{\delta}\} \qquad [28]$$

The variation in the number of cross-bridges formed can be found by using the chain rule, where:

$$dCB = \frac{\partial(CB)}{\partial(CB)_m} d(CB)_m + \frac{\partial(CB)}{\partial(CB)_a} d(CB)_a + \frac{\partial(CB)}{\partial\delta} d\delta + \frac{\partial(CB)}{\partial\dot{\delta}} d\dot{\delta} \qquad [29]$$

Denoting each of the partial differentials of CB by a transfer function K_i, we can write:

$$dCB = K_m d(CB)_m + K_a d(CB)_a + K_\delta d\delta + K_{\dot{\delta}} d\dot{\delta} \qquad [30]$$

where K_m, K_a, K_δ, and $\mathrm{K}_{\dot{\delta}}$ are the transfer functions for the system, which have yet to be developed.

Hatze (1981) models the number of cross-bridges formed as a function of the "active state", the degree of filamentary overlap, and the velocity of shortening or lengthening. He denotes N as the total number of cross-bridges in a half sarcomere, and Ω as the fraction of cross-bridges which are active at any given time, where Ω is given by:

$$\Omega = qk(\xi)J(\dot{\lambda}) \qquad [29]$$

q is related to the amount of Ca^{++} bound to TnC and is dependent on Hatze's relationships given by equations [4], [18], and [25]. The filamentary overlap function $k(\xi)$ is modelled as an exponential variation of the normalized length ξ and is empirically fit to the relationship of Gordon, et al. (1966). Hatze finds the relationship between force and velocity to be sigmoidal, and derives an expression for $H(\dot{\lambda})$ (where λ is the instantaneous length of the sarcomere) based on experimental evidence.

Hatze's derivation supplements the control system analysis very well. Its dependence on filamentary overlap and velocity of contraction can be represented as a feedback loop from the overall output of the muscle, δ and $\dot{\delta}$. The active state function q is simply a conglomeration of the control systems leading up to the development of $(CB)_m$ and $(CB)_s$. The output of the control system will thus be an active number of cross-bridges, CB.

Movement the of Cross-Bridge

The energy that is released by the ATP hydrolysis on the myosin head is thought to cause a deformation stress σ_d in the HMM subfragments. This deformation stress, u_d, disturbs the elastic cross-bridge and results in a deformation strain. As the cross-bridge (the controlled system) moves, the attached actin filament translates. The amount of translation and the strain in the cross-bridge affect the action of the restoring stresses u_c present in the system. The reference for the restoring mechanisms is the state of stress when the muscle is at rest, which should be equal to zero. These controlling systems include the inherent elasticity of the

cross-bridge, the inertial resistance of the molecules, the viscosity of the surrounding fluid, and opposing thermodynamic or electromagnetic fields which may exist. The binding force between the actin and the myosin will grow weaker as the connection between them is strained. The electromagnetic fields which we have assumed to cause the rotation will also decay as the field forces are changed. Finally, the dissociation mechanisms of relaxation (a new ATP on the myosin head and the uptake of Ca^{++}) will act to break the very bonds which form the cross-bridge. The output u of this system will be a characteristic deformation strain per cross bridge. This control system is shown if Figure 20.

It is generally agreed that the ATP hydrolyzed on the myosin head provides the energy for the contraction. However, there is a great deal of debate as to exactly how this chemical energy is transformed into mechanical work. Various theories include electrostatic repulsion and attraction, electromagnetic field effects, thermodynamic oscillations, and conformational changes. A historical overview of the proposed mechanisms of cross-bridge rotation and force generation is given in Appendix B.

One of the first models was proposed by A.F. Huxley (1957). He assumes a myosin-actin configuration as shown in Figure 21. The distance from the actin sites A to the myosin sites M is x, while the proportion of bonded sites is given as n. If the amount of energy released by the hydrolysis of one molecule of ATP for one contraction site $(A-M)$ is e, the overall chemical energy released is:

$$E = \frac{me}{l} \int_{-\infty}^{\infty} f(1-n)dx \qquad [30]$$

where l is the separation of A sites, and m is the number of M sites per cubic centimeter of muscle. The variable f is the rate of attachment of myosin and actin, which is a function of x, the distance between A and M. The average amount of work done per cross-bridge rotation (assuming a Hookean elastic element) is:

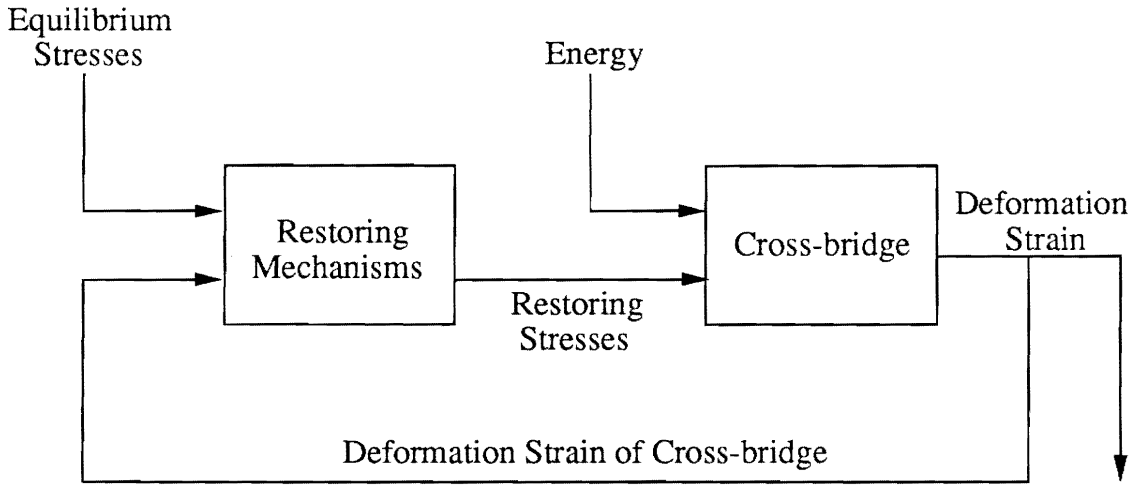

$$u_d = \sigma_d (ATP)$$

$$u_r = 0 \text{ stress at equilibrium}$$

$$u_c = \sigma_r (\varepsilon)$$

$$u: \quad E = \frac{m\,e}{L} \int_{-\infty}^{\infty} f(1-n)dx$$

$$W = \int_{-\infty}^{\infty} nkx\,dx$$

$$F_i = \frac{dG_i(x)}{dx}$$

Figure 20. Cross-bridge Movement: The controlled system is the cross-bridge, the controlling system the restoring mechanisms. u_d is the deforming stress resulting from the ATP hydrolysis, u_r is the equilibrium configuration of the cross-bridge, u_c is the restoring stresses, u is the deforming strain induced in the cross-bridge.

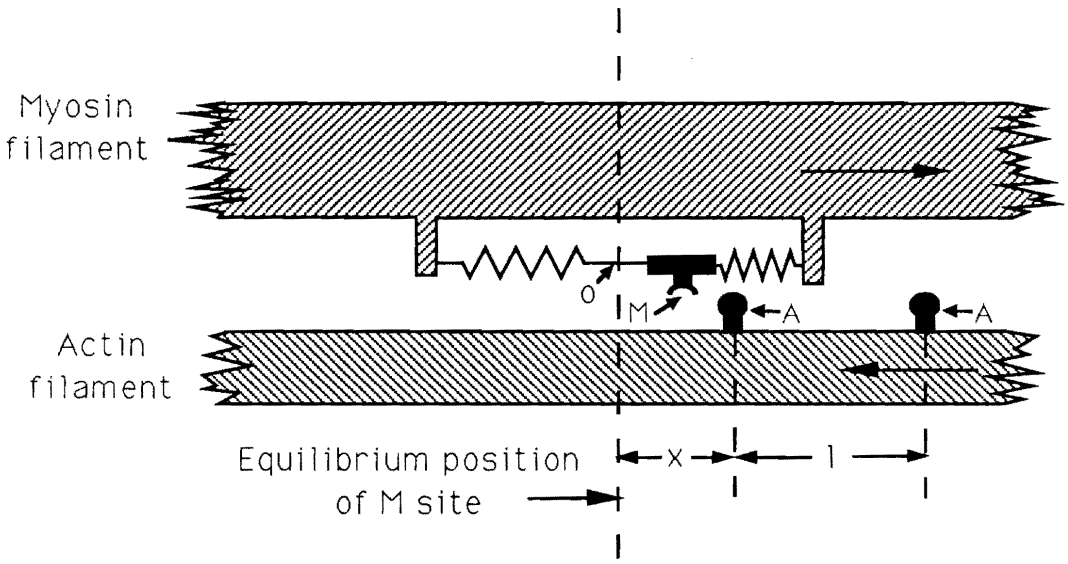

Figure 21. Huxley's Proposed Cross-Bridge Configuration: The model contains an elastic spring and depends on thermodynamic oscillations for a cross-bridge to form (after Huxley, 1957).

$$W = \int_{-\infty}^{\infty} nkxdx \qquad [31]$$

where k is the elastic spring constant of the cross-bridge, in dynes per centimeter. Huxley then empirically fits further calculations to match the data of A.V. Hill (1938). If these variables were actually able to be derived, equations [30] and [31] would fit nicely into the control diagram of Figure 20.

It has now become common to model the cross-bridge rotation as occurring in several discrete steps. It is thought that several different stable configurations of the cross-bridge exist, each with a different potential energy. The myosin head simply rotates from one configuration to one of lower potential energy, in the process releasing free energy which can be utilized as useful work. Such a process was described by Huxley and Simmons (1971) and is shown in Figure 22.

Pate and Cooke (1989) perform an elaborate analysis of such a cross-bridge scheme. They distinguish a finite number of stable configurations, each denoted by i, where $i = 1,2,...,m$ and m is the total number of configurations. Each configuration corresponds to a different step in the kinetics of the establishment of the cross-bridge, including the steps of ATP hydrolysis and products release. The force produced by a single cross-bridge in configuration i is a function of its Gibbs free energy, G_i. The distance between the binding sites, which is analogous to Huxley's x, is called the distortion, x_d. The force produced by a single cross-bridge in state i is given by:

$$F_i = \frac{dG_i(x_d)}{dx_d} \qquad [32]$$

This force is a response due to the hydrolysis of ATP, which causes a deforming stress σ_d. Pate and Cooke (1989) use a change in free energy due to the hydrolysis of ATP as $23RT$, where R is the universal gas constant and T is the absolute temperature in K. This yields a measurement of Joules per mole, which is a measure of the total free energy of contraction.

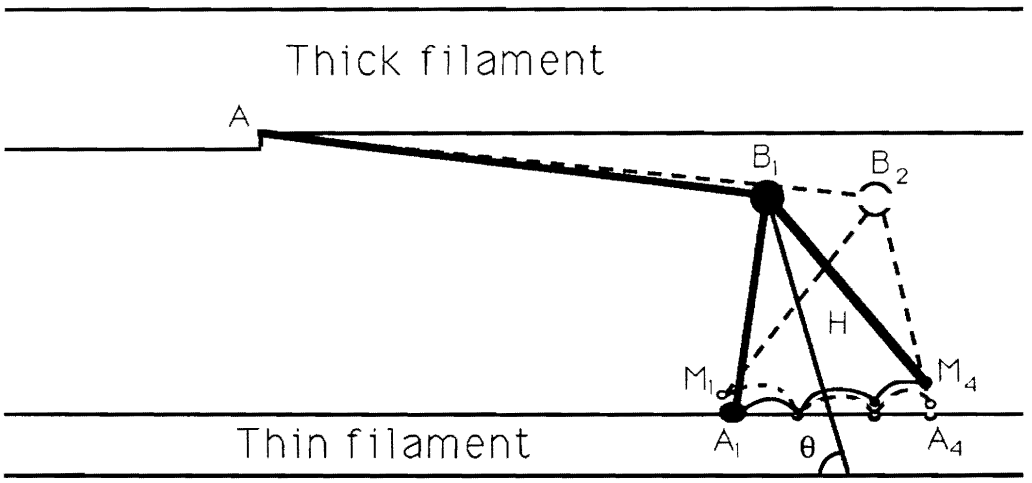

Figure 22. Cross-Bridge Proposed by Huxley and Simmons: The cross-bridge is assumed to rotate from one configuration to another of lower potential energy (from Huxley and Simmons, 1971).

The investigators then assume various free energy states of configurations i, and basically perform an empirical curve-fit to experimental data. The number and configuration of these steps is purely speculative, but describes a mechanism by which the contraction may take place. If these quantities can be determined, it will be possible to quantify the parameters of the cross-bridge power stroke control system.

Attempted Displacement of the Fiber

The total displacement developed by all of the cross-bridges is a function of the total number of cross-bridges *CB* and the amount of strain generated by each cross-bridge. This displacement then disturbs the resting architecture of the musculature to attempt to produce outputs of δ and $\dot{\delta}$. If there is no load or resistance on the muscle, the displacement of the fiber δ is equal to the attempted displacement δ_{att} of the cross-bridges. In this case the muscle undergoes a no-load, or atonic, contraction at maximum velocity $\dot{\delta}$. When the fiber attempts to contract against an external resistance, part or all of the "attempted" displacement is converted to a force. the displacement is converted to a force. This conversion to force is a result of the many cross-bridges which are present in the tissue, which act as scores of tiny force transducers in series. As the resistance approaches a maximum value, the "attempted" displacement becomes zero and the muscle experiences an isometric contraction, generating the largest force possible at zero speed.

The external load applied to the muscle, then, determines the total output of the muscle fiber. If the load is too high, the deformation stress σ_d is not capable of causing a strain. This is somewhat analogous to the case of thermal stresses, where the strain is zero if there is a constraint. The present analysis assumes a deformation strain ε_d which is then modulated due to the external load on the tissue. By superimposing these two effects, it is possible to obtain an output u. The overall output of the cross-bridges is an attempted displacement, which is transduced to a force if there is a load present. The output of the fiber combines this

cross-bridge output and the external resistance to produce a fiber displacement δ, a speed of contraction $\dot{\delta}$, a force F, and a time derivative of force $\dot{F}$. This corresponds to overall output u of Figure 10, and is the primary feedback signal u_p to the motor cortex.

Chapter IV - Summary and Conclusions

A constitutive control model describing active muscle contraction would be beneficial to all aspects of muscular research. To date only lumped-parameter, phenomenological approaches have been offered. These models do not consider the molecular events which are presently thought to occur in muscle, nor do they take into account the various controlling mechanisms inherent in the tissue. A proposed control model of these mechanisms has been discussed which might alleviate some of the problems of lumped-parameter analyses.

The current study has considered only simple, single-feedback loops (see Figure 9). The output of one control system becomes the input, or disturbing signal, for the next control system. The control systems are developed under the hypothesis that a contraction is a disturbance in the musculature; the tissue does not inherently *intend* to contract. Each controlling system is developed with the purpose of returning the controlled system to its equilibrium or resting configuration. In this fashion a cascading series of control systems is developed which closely matches the mechanisms of contraction. Proposed transfer functions for each model are discussed, as well as the connecting mechanisms from one system to the next.

After quantifying and establishing the transfer functions for each system, it will be possible to input variables which are different from those encountered in normally functioning

muscle. It may then be possible to determine the effects of various musculoskeletal diseases. Due to the systems approach undertaken, we may also be able to establish the locality of the adverse effects of these diseases.

Excitation of the muscle is fairly well understood. The aspects of synaptic transmission, as well as the propagation of the muscle action potential have benefitted from the vast amounts of neurological research performed. Researchers are just now experimenting with the mechanisms of excitation-contraction coupling. More accurate and more complex calcium compartmental models are being developed, and research is being conducted to establish the mechanics of the release of calcium by the sarcoplasmic reticulum cisterns.

There is still considerable debate as to the action of the calcium ions once they are released into the sarcoplasm. It is fairly well established that the binding of Ca^{++} to troponin-C sites exerts a regulatory effect on the generation of a contraction. Some researchers adhere to the steric blocking theory (see Figure 7), while others believe that the troponin-tropomyosin-actin configuration acts by altering the energy level of the ATP products on the myosin head. The establishment of any thick filament regulation in mammalian skeletal muscle is just now beginning to be considered.

Once past the regulatory mechanisms, the control model becomes somewhat speculative. This reflects the level of knowledge present in the field of myology today. The sliding-filament theory has withstood the test of time, yet scientists have been unable to determine the exact mechanisms by which it operates. Perhaps the control systems of Figures 17, 19 and 20 point towards the direction of future research.

An accurate, systematic controls analysis has been devised, offering a novel approach to quantifying muscle contraction. Transfer functions are developed where possible, and the framework for remaining systems is established. If these control systems can be quantified, it will be possible to input variables representing environments or diseased states not normally encountered by muscle tissue. Through experimentation or possibly through deriving approximate functions for these systems, it will be possible to quantify the entire model.

As Green (1969) stated, "if the characteristics of each subsystem and the rules for connecting one component to another were known, the problems would effectively be solved."

Appendix A. Control Diagrams

The standard feedback control system which is utilized in the project is shown in Figure 9. Its two main components are the controlled system and the controlling system. Each component has two primary inputs and a single output, which is a transfer function combining the effects of the two inputs. The inputs to the controlling system are the reference signal u_r and the feedback signal u_p. The reference signal is a set value which the controlling system "compares" to the feedback signal, and changes its output according to the difference between the two. This output is the control signal u_c, which is one of the inputs to the controlled system. The second input is some disturbing signal u_d. The output of each control system developed becomes the input to the succeeding system through this disturbing signal, u_d. This signal perturbs the control system from some initial state of equilibrium and initiates the control mechanisms described. Generally the control signal works to counteract the effects of the disturbing signal. The controlled system combines the actions of the disturbing signal and of the control signal and produces an output u. This output may then become the disturbing signal for a successive control system, or it may be the desired final outcome. It will also become a feedback signal u_p to the controlling system. In this way the controlling system will determine if the control it exerted over the controlled system (through u_c) was sufficient to return the system to its equilibrium configuration. This endless process of comparing

feedback signals to reference values is of utmost importance in the ability of living organisms to maintain homeostasis, and is accurately modelled by the system shown in Figure 9.

Appendix B. Cross-Bridge Force Generation

In 1954, the sliding filament theory of muscle contraction was proposed independently by two investigators. This theory involves two sets of interdigitating filaments which slide relative to one another, producing a shortening of the muscle. In two brief papers, A.F. Huxley and Nierdergerke (1954) and H.E. Huxley and Hanson (1954) revolutionized muscle research, and paved the way for much of what is currently known about muscular contraction.

To support the sliding filament model, there soon accumulated large amounts of evidence (see Huxley, 1980). It was found that actin and myosin existed separately (i.e. unattached) within the sarcomere. Previous models had conceptualized a continuous actomyosin strand which shortened upon activation. Many laboratories verified the Huxley observations that the A-band length remained essentially constant during contraction, while the I-band and H-zone shortened considerably. X-ray diffraction data revealed that there was not a large shift in mass distribution between the relaxed and the active states (see Squire, 1981). This discounted many theories which assumed major configurational changes of the contractile proteins. Finally, experiments on the length-tension relationship of sarcomeres (most notably by Gordon, et al. in 1966) fully supported the idea of sliding filaments.

The exact mechanism of this sliding became the subject of vast amounts of research. The length-tension data supported the theory of independent force generators; the force-

producing structures act as separate entities and not as a synchronous team. Further research suggested that these force generators were most probably the myosin heads (HMM S-1 and S-2), which were appropriately named cross-bridges. Investigators focused on two methods by which to classify the action of these cross-bridges. Mechanisms based on the kinetics of the biochemical processes involved yield valuable information on the behavior of the cross-bridge, while the second method, based on mechanical analysis, received its impetus from the classic work of A.F. Huxley (1957).

Huxley assumes the myosin molecule possesses an elastic sidepiece *M* which oscillates (due to thermal vibrations) about an equilibrium position. The sidepiece *M* is paired to an appropriate actin site *A* to which it will spontaneously bond. This configuration is shown schematically in Figure 21. The attachment of the actin to the myosin site is denoted by a function *f*, while the detachment is denoted by *g*. Both rates are given as functions of *x*, the distance between *A* and *M*.

The functions that Huxley assigns to *f* and *g* are shown in Figure 23. He assumes that some endergonic reaction must cause the detachment of the A-M complex, and that this would only occur during "negative" displacements. The detachment might be due to some enzymatic breakdown of the A-M complex and that enzyme could be located in a vicinity where the strain is negative (i.e. just to the left of *M*). Huxley assumes that the energy of contraction is supplied by the positioning of a high-energy phosphate compound on the actin site. It is amazing that this hypothesis was quite close to the present theory that ATP binding to the myosin head generally causes detachment of the actomyosin complex (see Huxley, 1980).

Huxley then proceeds to develop a mathematical description of his model, with the goal of replicating the findings of Hill (1938) and of experimental length-tension data. Huxley denotes the proportion of sites where *M* is bonded to *A* by *n*, from which he obtains:

$$\frac{\partial n}{\partial t} = (1 - n)f - ng \qquad [33]$$

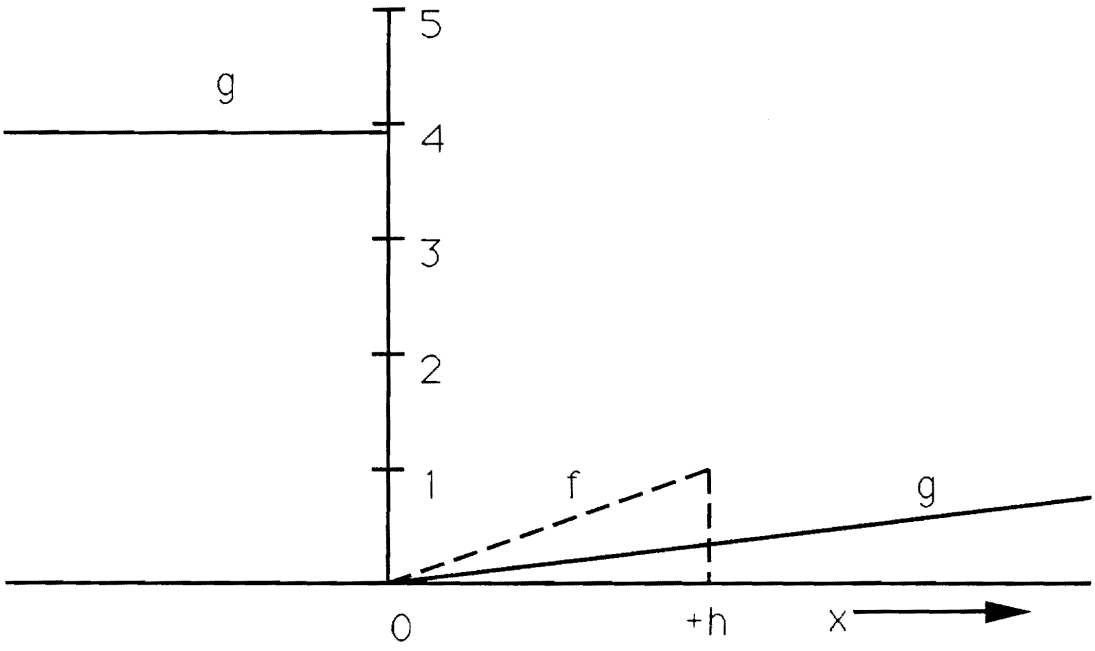

Figure 23. Huxley's Rate Constants: The dissociation function *g* only takes on non-zero values when it performs negative work. The binding function, *f*, varies linearly with *x* until some maximum distance *h* (from Huxley, 1957).

Huxley then derives a relationship for energy liberation per cubic centimeter of muscle as

$$E = \frac{me}{l} \int_{-\infty}^{\infty} f(1-n)dx \qquad [34]$$

where e is the amount of ergs per contraction site liberated by one the hydrolysis of one molecule of ATP, l is the separation of A sites, and m is the number of M sites per cubic centimeter of muscle. The average amount of work done per cross-bridge rotation (assuming a Hookean elastic element) is:

$$W = \int_{-\infty}^{\infty} nkxdx \qquad [35]$$

where k is the elastic spring constant of the cross-bridge. Denoting s as the sarcomere length, the tension per square centimeter of muscle can be derived as:

$$P = \frac{msk}{2l} \int_{-\infty}^{\infty} nxdx \qquad [36]$$

Utilizing equations [33], [34], [35], and [36] and inserting his values for f and g, Huxley was able to obtain expressions for "maintenance heat" rate, the "extra rate of energy liberation", tension, and the rate of doing mechanical work. Huxley's results match the work of A.V. Hill (1938) remarkably well.

This work stimulated the efforts of other muscle researchers to test Huxley's results. Several authors (see Squire, 1981) modified Huxley's attachment and detachment constants to better match new experimental findings. As the experimental equipment became more sophisticated, further advances were made upon Huxley's original idea. Smaller time scales

were imposed on the step-displacement and step-tension tests, which revealed that the muscle exhibited a four-phase response (shown in Figure 24).

Huxley and Simmons (1971) were the first to attempt to model these responses phenomenologically. The first phase is an instantaneous elasticity, which may be present in the cross-bridges themselves or in series elastic elements (elastic tissue in the myofibrils). During the next 1-2 msec, there is a rapid tension recovery. Then in phase 3, there is an extreme reduction of this recovery rate, and a gradual return to an asymptotic value of tension in phase 4. These final three phases are thought to be due to different attachment cycles of the cross-bridges. Huxley and Simmons propose that the behavior of the muscle is best described using two structural elements in series; a pure elastic element thought to reside in the cross-bridges, and a viscoelastic element which could account for the nonlinear tension recovery period. They apply theories of high molecular weight polymers to describe the latter element.

The authors make two primary assumptions. The first is that the cross-bridge undergoes a series of transitions from one stable configuration to another stable configuration of lower potential energy. During this transition, the cross-bridge performs work. The second assumption is that an intrinsic elasticity within the cross-bridges prevents the entire thin filament from displacing relative to the thick filament during phase 1. A diagram of the proposed cross-bridge mechanism is shown in Figure 22. The S-2 head is assumed to possess the instantaneous elasticity shown in phase 1. A single rotational degree of freedom is assumed, with the cross-bridge rotating from low-strength actomyosin bonds to high-strength actomyosin bonds. The attachment of an ATP molecule to the myosin head would then cause detachment of the cross-bridge. Huxley and Simmons propose various potential diagrams for these positions, including the energy added by the hydrolysis of the ATP on the S-2 unit.

Once again, A.F. Huxley set a standard for other investigators. Many models were established which utilized the idea of potential energy curves. Although other authors had applied the idea to muscle contraction, none had coupled the potential energy curves so closely to the mechanical events which were thought to occur.

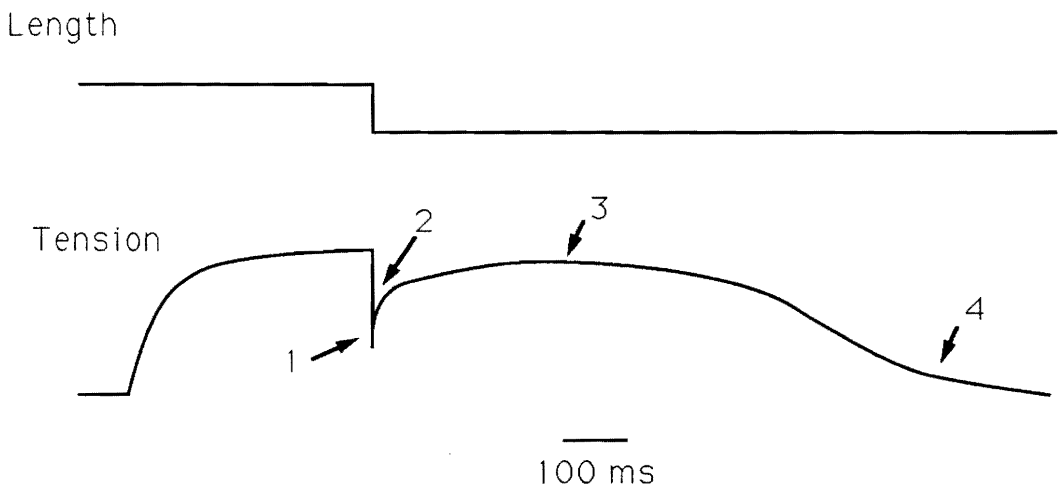

Figure 24. Characteristic Time-Tension Relationships: Described as having four phases by Huxley and Simmons, denoted on the figure (after Huxley and Simmons, 1971).

A more complex mechanism for cross-bridge action is proposed by Hatze (1973). He suggests that only one of the HMM S-1 globular heads is capable of moving, while the one most distal to the HMM S-2 rod is assumed to remain relatively rigid. Strong intermolecular forces maintain an equilibrium position for the two subunits, which Hatze calculates to be about eight degrees (see Figure 25(a)). When calcium is released from the sarcoplasmic reticulum cisterns, he postulates, it causes a decrease in the electrical resistance of the troponin-C, tropomyosin, and the actin monomer. The calcium also binds to the top of the myosin ATP binding site and aids in the hydrolysis of the ATP molecule. This results in a negatively-charged myosin head, which establishes a potential difference between the myosin and the actin. The HMM subfragments are then electrically attracted to the actin, and the mobile HMM S-1 is able to bond to an actin site. This results in an electrical current, which travels through a large array of charge-paths. An oscillating magnetic field is established, which generates a mechanical force in the presence of an electric current. This force causes the mobile globular head to separate from the rigid head. Due to the attachment of the mobile head to the actin, a relative motion occurs. This series of events is shown in Figure 25.

Hatze then suggests that the motion of the HMM S-1 results in a decrease in the electrical field. He hypothesizes that the bond strength of the actomyosin complex is a function of the electrical field, and that this bond breaks when the electrical field passes through its zero phase. After detachment, the mobile HMM S-1 is said to return to its equilibrium configuration. The magnetic field now also declines, and "transfers its energy content to the electrical energy depot". He further assumes that this process then repeats until the energy of the hydrolyzed ATP molecule is exhausted. The cyclic action is calculated to cause a displacement of 2 Angstroms per oscillation.

Hatze then performs a complicated mathematical formulation of his model, calculating inductance and several energy functions. His model seems far-fetched, and lacks any true experimental evidence to verify his lofty assumptions. No investigator has found such a connection of the HMM S-1 subunits to exist, and Hatze declines to explain the details of his magical electrical energy depot. He admits that the model is highly speculative, but maintains

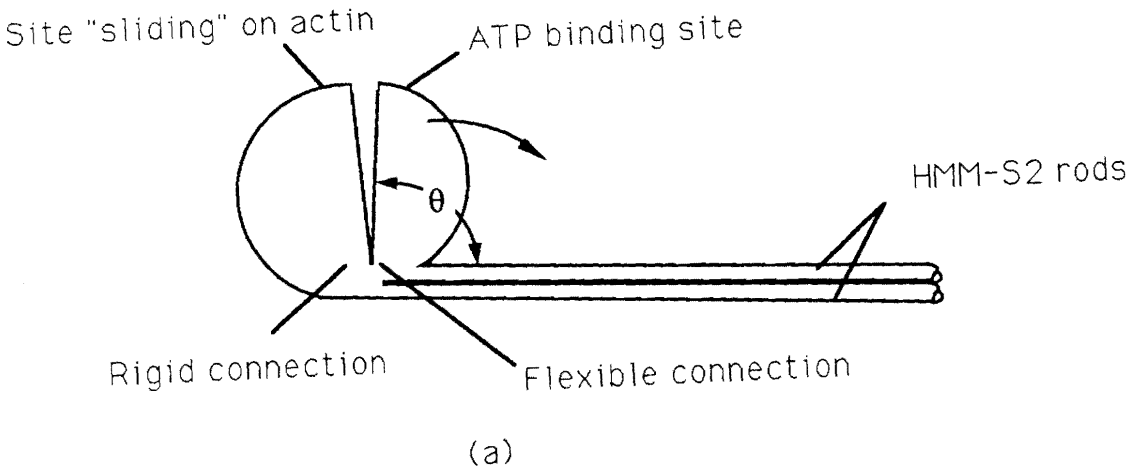

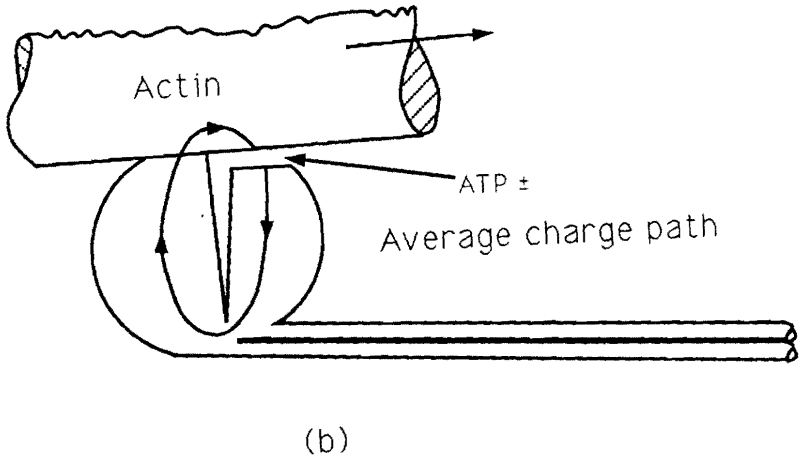

Figure 25. Cross-Bridge Proposed by Hatze: (a) Only one portion of the myosin head is assumed to be able to move, and (b) the power stroke is a result of complex electromagnetic fields (from Hatze, 1973).

that it is conceivable. The accurate results his model attains provide him with a small air of success, but the equations seem to have simply been empirically fit using several variable parameters. To his credit, Hatze has ventured farther into the molecular mechanics than any other author to date, attempting to explain the exact nature of the cross-bridge mechanism.

Another approach which is different from most investigators is that of Harrington (1979). He studies the "rate of unfolding the two-stranded coiled-coil of the alpha helices in the S-2 region of rabbit skeletal myosin" (Harrington, 1979, p. 5066). The relaxation times for this occurrence are very similar to those of recovering muscle. Harrington proposes that the shortening element, as well as the series elastic element, is present in the HMM S-2 subunit. In the resting state, the S-2 is thought to be bound to the LMM. When the attached HMM S-1 subunit binds to the actin molecule, however, the HMM S-2 raises up. A segment of the S-2, thought to be one-third to one-half its length, transforms from an alpha-helix into a coil. This "melting" results in a shortening of the myosin head, and the actin slides with respect to the myosin filaments. This is shown schematically in Figure 26. At the same time the S-1 subunit rotates slightly, acting as a tension-absorbing spring. The S-2 will maintain a dynamic equilibrium between the coiled and the alpha-helix regions during an isometric contraction.

Harrington calculates the force generated when the S-2 region is fully coiled to be

$$f = BTL[1 - (\frac{L_i}{L})^3]$$

L_i is the isotropic length of the force-generating S-2 segment, T is the absolute temperature, L is the end-to-end length of the coil, and B is a function of the polypeptide elements in the chain. He derives several other formulas which are developed using polymer kinetics and energy releases, and ultimately yields results that are significantly different from experimental evidence. The average isometric force per cross-bridge is given as 1.5 to 1.7 x 10^{-12}N, which is equivalent to a maximal contraction of 1.4 to 2.0 x 10^5 N per square meter. This is only one-half the maximum tension developed by frog sartorius muscle, and Harrington assumes that all of the cross-bridges in the thick filament are attached. He notes that his model as-

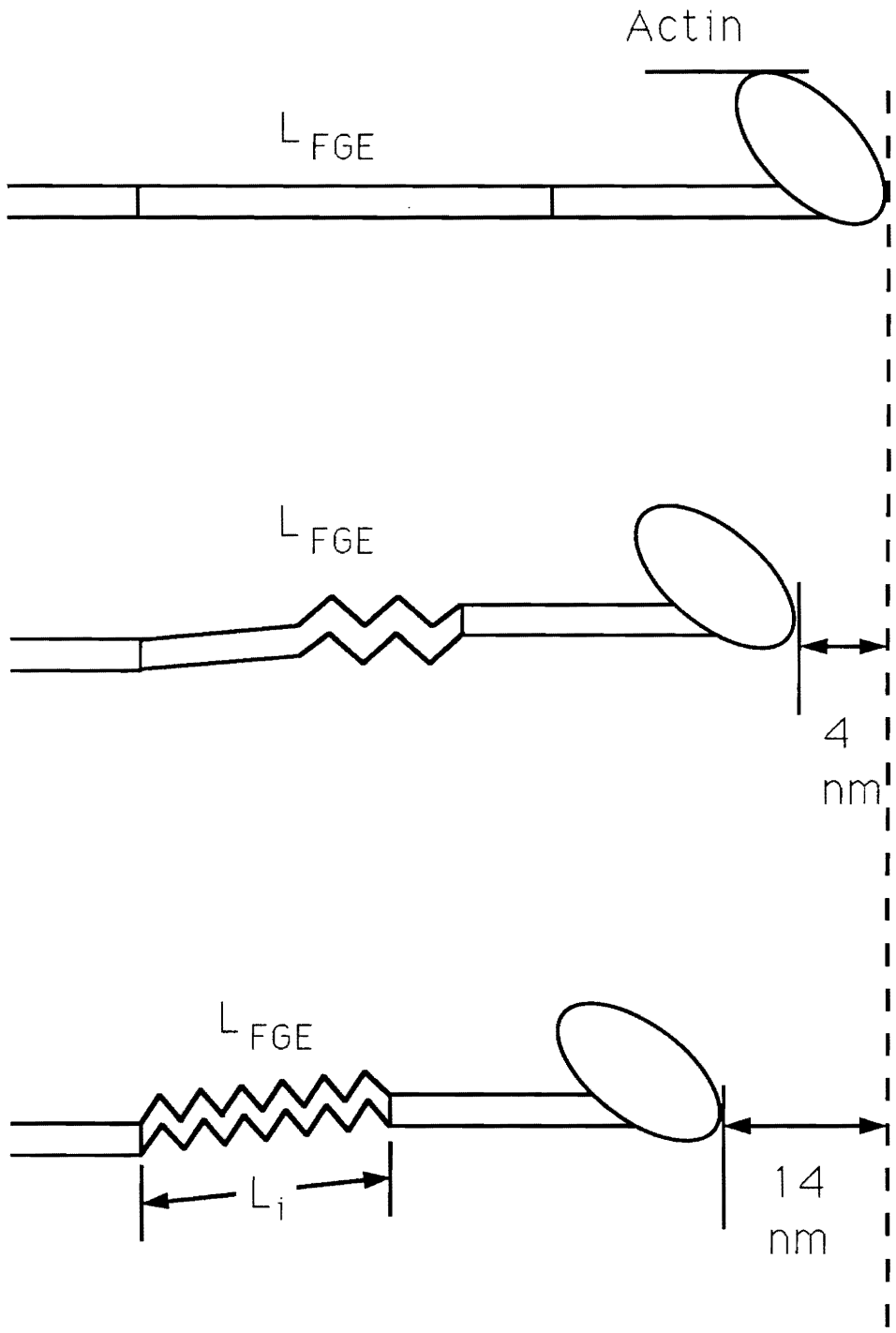

Figure 26. Cross-Bridge Proposed by Harrington: The alpha helical coil of the HMM S-2 region is said to "melt", causing the length of the myosin head to become shorter (from Harrington, 1979).

sumes a one-component (homopolymer) system. Some parameters might also be manipulated to provide better results. To date his hypothesis has not been disproven, and is the most feasible alternative to the rotating cross-bridge theories.

The previous cross-bridge theories have all been predominantly based on mechanical events which occur during contraction. A second approach to studying contraction is by using biochemical data. These experiments are all performed in solution, so there is some question as to whether the results can be applied to muscle in vivo. Several investigators have determined that this is probably valid (see Pate and Cooke, 1989). Lymm and Taylor (1971) performed early experiments on the kinetics of ATP hydrolysis. By using a rapid-mixing apparatus, they were able to isolate steps of interaction between actin, myosin, and ATP and its dissociation products. The actomyosin becomes rapidly detached when ATP becomes bound to the myosin head. While the ATP is hydrolyzed, the cross-bridge returns to its equilibrium position. Now in the vicinity of actin, the cross-bridge can be formed. As the products are released, force is generated. Then another ATP molecule is thought to bond to the myosin, initiating a new cycle.

Many authors have explored the ATPase kinetics. T.L. Hill (1974) performed an extensive analysis of the thermodynamic properties of the ATP kinetic cycle. Eisenberg et al (1980) propose a kinetic scheme which is closely coupled to mechanical events. Pate and Cooke (1988) expand and modify these findings. They propose a mechanism that drives the cross-bridge process by free-energy obtained from the hydrolysis of ATP. A series of five states is used to model the chemical and mechanical configurations of the cross-bridge, as shown in Figure 27.

The free-energy of each kinetic state is modelled as a function of x_d, the distance between a binding site on myosin and a site on a neighboring actin monomer. The force produced by a certain state is then the spatial derivative of this energy. A detached cross-bridge has no free-energy, and thus generates no force. If n_i is the fraction of cross-bridges in a given state i, then the force per unit length of filament overlap is computed to be

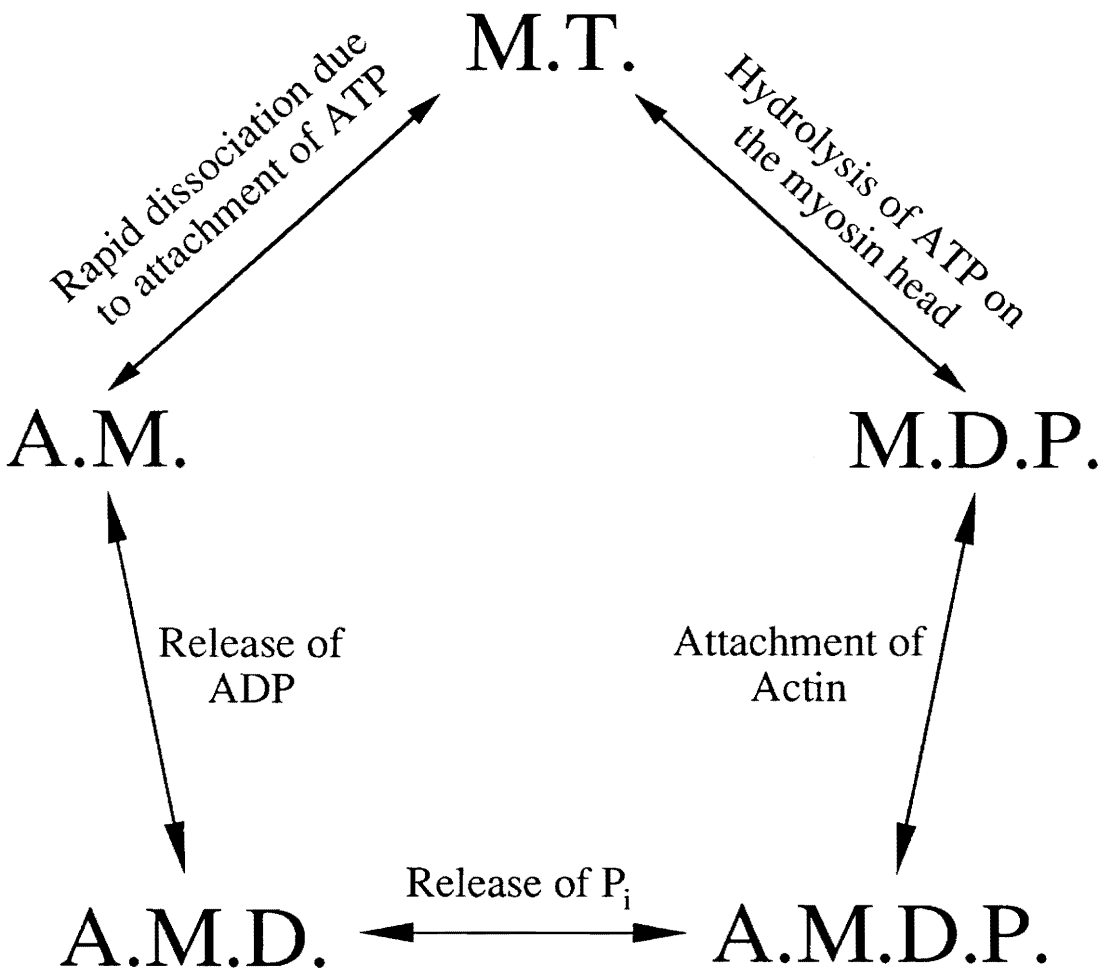

Figure 27. Cross-Bridge States Proposed by Pate and Cooke: The chemical states of the cross-bridge, where *A* denotes actin, *M* denotes myosin, *D* is ADP, *T* is ATP, and *P* is inorganic phosphate (after Pate and Cooke, 1989).

$$F = \frac{1}{b-a} \int_{-\infty}^{\infty} \sum_{i=1} n_i(x) F_i(x) dx$$

F_i is the work done by the free energy in state i, and the cross-bridge only forms if x_d is between a and b. Parabolic free energy curves are obtained as functions of x_d and shown in Figure 28.

As evident by Figure 28, there is a weakly bound actin-myosin-ADP-phosphate state which transitions to a strongly bound actin-myosin-ADP state upon release of the inorganic phosphate. The force is primarily generated in this actin-myosin-ADP state. As the force-generating capabilities decrease the ADP molecule is released, allowing a new molecule of ATP to bond to the myosin head, causing detachment. This kinetic study was coupled to data which relates the maximum velocity of shortening and the maximum tension to concentrations of various ligands. Pate and Cooke were able to successfully match experimental data relating kinetic and mechanical data.

Many other variations have been offered to explain muscle contraction. McClare (1972) proposes a quantum mechanical muscle model. He suggests that the hydrolysis of ATP causes a resonant vibration of the proteins present, and an electromagnetic coupling occurs. Squire (1981) presents a scheme similar to that of Pate and Cooke. Vaccaro et al. (1989) suggest that nonlinear effects are not being properly included in the cross-bridge models.

The accumulation of models has occurred because none to date has proven to be satisfactory. Most of the research indicates that the answer will come through coupling mechanical studies with ATP kinetic schemes. The cross-bridges are so small (around 15 nm long and 5 nm wide) that it is difficult to obtain structural data. Biochemical data is also difficult to obtain; there are numerous protein structures, and it is presently impossible to determine the exact state of a particular cross-bridge. There is even a chance that the cross-bridges have nothing whatsoever to do with muscle contraction. At the present time, however, most experimental work seems to support the independent force generator, sliding filament theory of muscle contraction.

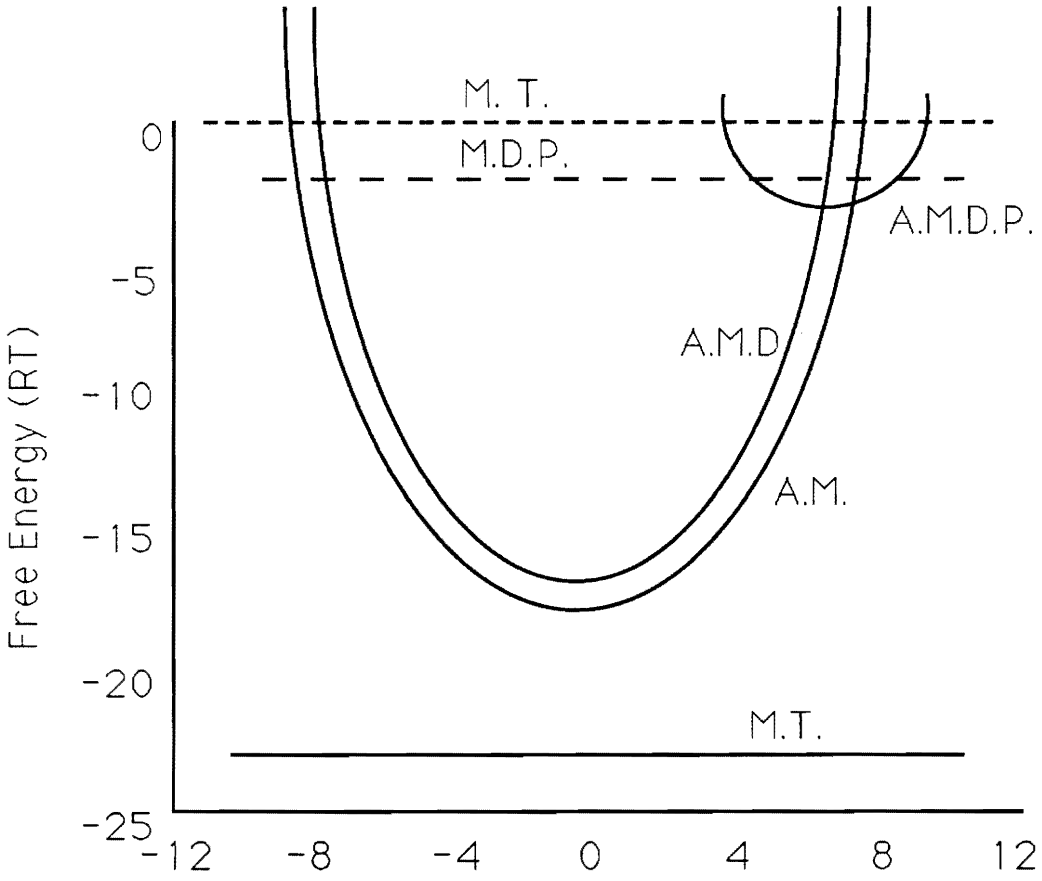

Figure 28. Potential Energy Diagrams of Cross-Bridge Configurations: The potential energy curves of the cross-bridge states, where *A* denotes actin, *M* denotes myosin, *D* is ADP, *T* is ATP, and *P* is inorganic phosphate (from Pate and Cooke, 1989).

References

Bahler, A. (1968), "Modeling of Mammalian Skeletal Muscle", *IEEE Transactions on Bio-Medical Engineering*, Vol. BME-15, No.4, pp. 249-257.

Bagshaw, C.R. (1982), *Muscle Contraction*, New York, Chapman and Hall.

Bawa, P., Mannard, A., and Stein, R. (1976), "Predictions and Experimental Tests of A Visco-Elastic Muscle Model Using Elastic and Inertial Loads", *Biological Cybernetics*, Vol. 22, pp. 139-145.

Bendall, J. (1969), *Muscles, Molecules and Movement*, New York, American Elsevier.

Bendat, J. and Piersol, A. (1971), *Random Data: Analysis and Measurement Procedures*, New York, Wiley-Interscience.

Cannell, M. and Allen, D. (1984), "Model of Calcium Movements During Activation in the Sarcomere of Frog Skeletal Muscle", *Biophysics Journal*, Vol. 45, pp 913-925.

Cohen, C. (1975), "The Protein Switch of Muscle Contraction", *Scientific American*, Vol. 233, No. 5, pp. 36-45.

Cooke, R. (1986), "The Mechanism of Muscle Contraction", *CRC Critical Reviews in Biochemistry*, Vol. 21, pp. 53-118.

Dayhoff, J. (1990), "Pulse Transmission Neural Networks", In: Mikulecky, D.C. and Clarke, A.M. (editors), *Biomedical Engineering: Opening New Doors*, New York, New York University Press, pp. 265-274.

Eisenberg, E., Hill, T., and Chen, Y (1980), "Cross-bridge Model of Muscle Contraction", *Biophysics Journal*, Vol. 29, pp. 195-227.

Endo, M. (1977), "Calcium Release from the Sarcoplasmic Reticulum", *Physiological Reviews*, Vol. 57, No. 1, pp 71-108.

FitzHugh, R. (1977), "A Model of Optimal Voluntary Muscular Control", *Journal of Mathematical Biology*, Vol. 4, pp. 203-236.

Gergely, J. (1976), "Mechanism of Muscle Contraction", In: Rao Sanadi, R. (editor), *Chemical Mechanisms in Bioenergetics*, Washington, D.C., American Chemical Society, pp. 221-262.

Gillis, J.M., Thomason, D., LeFevre, J. and Kretsinger, R.H. (1982) "Parvalbumins and Muscle Relaxation: A Computer Simulation Study", *Journal of Muscle Research and Cell Motility*, Vol. 3, pp.377-398.

Gordon, A., Huxley, A.F. and Julian, F. (1966), "The Variation in Isometric Tension with Sarcomere Length in Vertebrate Muscle Fibers", *Journal of Physiology*, Vol. 184, pp. 170-192.

Green, D. (1969), "A Note on Modelling Muscle in Physiological Regulators", *Medical and Biological Engineering*, Vol. 7, pp. 41-48.

Guyton, A. (1986), *Textbook of Medical Physiology*, Philadelphia, Pennsylvania, W.B. Saunders Company.

Harrington, W. (1979), "On the Origin of the Contractile Force in Skeletal Muscle", *Proceedings of the National Academy of Science, USA*, Vol. 76, No. 10, pp. 5066-5070.

Hatze, H. (1973), "A Theory of Contraction and a Mathematical Model of Striated Muscle", *Journal of Theoretical Biology*, Vol. 40, pp. 219-246.

Hatze, H. (1981), *Myocybernetic Control Models of Skeletal Muscle*, Pretoria, South Africa, University of South Africa.

Hill, T. (1974), "Theoretical Formalism for the Sliding-filament Model of Contraction of Striated Muscle, Part I", *Progress in Biophysics and Molecular Biology*, Vol. 28, pp. 267-340.

Hill, A.V. (1938), "The Heat of Shortening and the Dynamic Constants of Muscle", *Proceedings of the Royal Society of London, Series B*, Vol. 126, pp. 136-195.

Hoffman, P., Metzger, J., Greaser, M., and Moss, R. (1990), "Effects of Partial Extraction of Light Chain 2 on the Ca^{2+} Sensitivities of Isometric Tension, Stiffness, and Velocity of Shortening in Skinned Skeletal Muscle Fibers", *Journal of General Physiology* , Vol. 95, pp. 477-498.

Huxley, A.F. (1980), *Reflections on Muscle*, Liverpool, England, Liverpool University Press.

Huxley, A.F. (1957), "Muscle Structure and Theories of Contraction", In: Butler, E. and Katz, B. (editors), *Progress in Biophysics and Biophysical Chemistry*, Vol. 7, pp. 255-318.

Huxley, A.F. and Niedergerke, R. (1954), "Structural Changes in Muscle During Contraction", *Nature*, Vol. 173, pp. 971-972.

Huxley, A.F. and Simmons, M. (1971), "Proposed Mechanism of Force Generation in Striated Muscle", *Nature*, Vol. 233, pp. 533-538.

Huxley, H.E. and Hanson, E. (1954), "Changes in the Cross-Striations of Muscle During Contraction and Stretch and Their Structural Interpretation", *Nature*, Vol. 233, pp. 533-538.

Jobsis, F. and O'Connor, M. (1966), "Calcium Release and Reabsorption in the Sartorius Muscle of the Toad", *Biochemical and Biophysical Research Communications*, Vol. 25, No. 2, pp. 246-252.

Lymm, R. and Taylor, E. (1971), "Mechanism of Adenosine Triphosphate Hydrolysis by Actomyosin", *Biochemistry*, Vol. 10, No. 25, pp. 4617-4624.

McClare, C. (1972), "A Quantam Mechanical Muscle Model", *Nature*, Vol. 240, pp. 88-90.

Mezler, W., Rios, E. and Schneider, M. (1984), "Time Course of Calcium Release and Removal in Skeletal Muscle Fibers", *Biophysics Journal*, Vol. 45, pp. 637-641.

Nubar, Y. (1962), "Stress-Strain Relationship in Skeletal Muscle", *Annals of the New York Academy of Sciences*, Vol. 93, pp. 857-876.

Pate, E. and Cooke, R. (1989), "A Model of Crossbridge Action: The Effects of ATP, ADP and P_i ", *Journal of Muscle Research and Cell Motility*, Vol. 10, pp. 181-196.

Plonsey, R. (1969) *Bioelectric Phenomena*, New York, McGraw-Hill Book Company.

Reedy, M., Holmes, K., and Treglar, R. (1965), " Induced Changes in Orientation of the cross-bridges of glycerinated insect flight muscle" *Nature*, Vol. 207, pp. 1276-1280.

Rios, E. and Gonzalo, P. (1988), "Voltage Sensors and Calcium Channels of Excitation-Contraction Coupling", *News in Physiological Sciences*, Vol. 3, pp. 223-227.

Robertson, S., Johnson, J., and Potter, J. (1981), "The Time-Course of Ca^{2+} Exchange with Calmodulin, Troponin, Parvalbumin, and Myosin in Response to Transient Increases in Ca^{2+}", *Biophysics Journal*, Vol. 34, pp 559-569.

Schneck, D. J. (1990), *Engineering Principles of Physiologic Function*, New York, The New York University Press.

Schneck, D. J. (1991), *Mechanics of Muscle*, New York, The New York University Press, (in production).

Sperelakis, N. and Fabiato, A. (1985), "Electrophysiology and Excitation-Contraction Coupling in Skeletal Muscle", In: Roussos, C. and Macklem (editors), *Lung Biology in Health and Disease*, Vol. 29, pp. 45-113.

Squire, J. (1981), *The Structural Basis of Muscular Contraction*, New York, Plenum Press.

Squire, J. (1986), *Muscle- Design, Diversity, and Disease*, Reading, Massachusetts, Benjamin/Cummings.

Squire, J., editor (1990), *Molecular Mechanisms in Muscular Contraction*, Boca Raton, CRC Press, Inc.

Vaccaro, D., Agarwal, G., and Gottlieb, G. (1988), "Nonlinear Mechanical Behavior in Striated Muscle and Its Relationship to Underlying Crossbridge Activity", *IEEE Transactions on Biomedical Engineering*, Vol. 35, No. 6, pp. 426-434.

Williams, W. and Edwin, A. (1970), "An Electronic Muscle Simulator for Demonstration and Neuromuscular Systems Modelling", *Medical and Biological Engineering*, Vol. 8, pp. 521-524.

Woledge, R., Curtin, N. and Homsher, E. (1985), *Energetic Aspects of Muscle Contraction*, Orlando, Florida, Academic Press, Inc.

The vita has been removed from the scanned document